nagra
National Cooperative for the
Disposal of Radioactive Waste

TECHNICAL REPORT 99-09

Coupled Transport Phenomena in the Opalinus Clay: Implications for Radionuclide Transport

September 1999

J.M. Soler

PSI, Würenlingen and Villigen

Hardstrasse 73, CH-5430 Wettingen/Switzerland, Telephone +41-56-437 11 11

nagra
National Cooperative for the
Disposal of Radioactive Waste

TECHNICAL REPORT 99-09

Coupled Transport Phenomena in the Opalinus Clay: Implications for Radionuclide Transport

September 1999

J.M. Soler

PSI, Würenlingen and Villigen

Hardstrasse 73, CH-5430 Wettingen/Switzerland, Telephone +41-56-437 11 11

This report was prepared on behalf of Nagra. The viewpoints presented and conclusions reached are those of the author(s) and do not necessarily represent those of Nagra.

PREFACE

The Laboratory for Waste Management at the Paul Scherrer Institut is performing work to develop and test models as well as to acquire specific data relevant to performance assessments of planned Swiss nuclear waste repositories. These investigations are undertaken in close co-operation with, and with the financial support of, the National Co-operative for the Disposal of Radioactive Waste (Nagra). The present report is issued simultaneously as a PSI-Bericht and a Nagra Technical Report.

ISSN 1015-2636

ABSTRACT

Coupled phenomena (thermal and chemical osmosis, hyperfiltration, coupled diffusion, thermal diffusion, thermal filtration, Dufour effect) may play an important role in fluid, solute and heat transport in clay-rich formations, such as the Opalinus Clay (OPA), which are being considered as potential hosts for radioactive waste repositories. In this study, the potential effects of coupled phenomena on radionuclide transport in the vicinity of a repository for vitrified high-level radioactive waste (HLW) and spent nuclear fuel (SF) hosted by the Opalinus Clay, at times equal to or greater than the expected lifetime of the waste canisters (about 1000 years), have been addressed.

Firstly, estimates of the solute fluxes associated with chemical osmosis, hyperfiltration, thermal diffusion and thermal osmosis have been calculated. Available experimental data concerning coupled transport phenomena in compacted clays, and the hydrogeological and geochemical conditions to which the Opalinus Clay is subject, have been used for these estimates. These estimates suggest that thermal osmosis is the only coupled transport mechanism that could have a strong impact on solute and fluid transport in the vicinity of the repository.

Secondly, estimates of the heat fluxes associated with thermal filtration and the Dufour effect in the vicinity of the repository have been calculated. The calculated heat fluxes are absolutely negligible compared to the heat flux caused by thermal conduction.

As a further step to obtain additional insight into the effects of coupled phenomena on solute transport, the solute fluxes associated with advection, chemical diffusion, thermal and chemical osmosis, hyperfiltration and thermal diffusion have been incorporated into a simple one-dimensional transport equation. The analytical solution of this equation, with appropriate parameters, shows again that thermal osmosis is the only coupled transport mechanism that could have a strong effect on repository performance, in agreement with the previous estimates.

Finally, the results of two- and three-dimensional simple flow models incorporating advection (Darcy's law) and thermal osmosis show that, under the conditions in the vicinity of the repository at the time scales of interest, the advective component of flow will oppose and cancel the thermal-osmotic component.

After evaluating the different coupled transport mechanisms, the conclusion is that coupled phenomena will only have a very minor impact on radionuclide transport in the Opalinus Clay, at least under the conditions at times equal to or greater than the expected lifetime of the waste canisters (about 1000 years).

ZUSAMMENFASSUNG

Gekoppelte Prozesse (thermische und chemische Osmose, Hyperfiltration, gekoppelte Diffusion, thermische Diffusion, thermische Filtration, Dufour-Effekt) können eine wichtige Rolle spielen beim Transport von Wasser, Wasserinhaltsstoffen und Wärme durch tonreiche Formationen, wie z.B. den Opalinuston (OPA), welche als mögliche Wirtsgesteine für eine Endlager für radioaktive Abfälle angesehen werden. In der vorliegenden Studie werden die möglichen Auswirkungen der gekoppelten Prozesse auf den Radionuklid-Transport in der Nähe eines im Opalinuston gelegenen Endlagers für verglaste hoch-radioaktive Abfälle (HLW) und abgebrannte Brennelemente (SF) angesprochen für Zeiten die gleich oder grösser als die erwartete Lebensdauer der Abfallkanister (ca. 1000 Jahre) sind.

Zuerst wurden die Flüsse für Wasserinhaltsstoffe als Folge von chemischer Osmose, Hyperfiltration, thermischer Diffusion und thermischer Osmose abgeschätzt. Dazu wurden verfügbare experimentelle Daten bezüglich gekoppelter Transportprozesse in kompaktierten Tonen, unter Berücksichtigung der hydrogeologischen und geochemischen Bedingungen des Opalinustons, verwendet. Diese Abschätzungen legen den Schluss nahe, dass nur die thermische Osmose als einziger der gekoppelten Transportmechanismen einen wesentlichen Einfluss auf den Stofftransport und den Transport von Wasser in der Nähe eines Endlagers haben könnte.

In einem zweiten Schritt wurden Abschätzungen vorgenommen für den Wärmefluss in der Nähe eines Endlagers als Folge von thermischer Filtration und des Dufour-Effekts. Die berechneten Wärmeflüsse sind aber komplett vernachlässigbar zu demjenigen der Wärmeleitung.

Um einen weiteren Einblick in die Auswirkungen der gekoppelten Prozesse auf den Stofftransport zu erhalten, wurden in einem weiteren Schritt die Flüsse als Folge von Advektion, chemischer Diffusion, thermischer und chemischer Osmose, Hyperfiltration und thermischer Diffusion mittels einer einfachen ein-dimensionalen Transportgleichung berechnet. Die analytische Lösung dieser Gleichung, mit geeigneten Parametern, zeigt wiederum und in Übereinstimmung mit vorangehenden Abschätzungen, dass die thermische Osmose der einzige gekoppelte Transport-Mechanismus ist, welcher starke Auswirkungen auf das Systemverhalten eines Endlagers haben könnte.

Schliesslich zeigen die Ergebnisse im Rahmen eines einfachen zwei- und drei-dimensionalen Fliessmodells unter Berücksichtigung von Advektion (Darcy-Gesetz) und thermischer Osmose, dass - unter den Bedingungen, die in der Nähe eines Endlagers herrschen - für die interessierenden Zeitskalen, die advektive Komponente des Flusses derjenigen der thermischen Osmose entgegengesetzt ist und diese kompensiert.

Die Auswertung der verschiedenen gekoppelten Transportmechanismen lässt den Schluss zu, dass gekoppelte Prozesse nur einen sehr beschränkten Einfluss auf den Radionuklid-Transport im Opalinuston haben werden, unter

der Bedingung, dass die Zeiten vergleichbar oder grösser sind als die erwartete Lebensdauer der Abfallkanister (ca. 1000 Jahre).

RESUME

Les phénomènes couplés (osmose thermique et chimique, hyperfiltration, diffusion couplée, diffusion thermique, filtration thermique et effet Dufour) sont susceptibles de jouer un rôle important au niveau des mécanismes d'écoulement de transport de solutés et de chaleur dans les formations riches en argiles, telles que les argiles à Opalines (OPA). Ces formations sont considérées comme des roches d'accueil potentielles pour le confinement des déchets radioactifs. Dans ce travail, les effets potentiels de phénomènes couplés sur le transport de radionucléides ont été étudiés au voisinage d'un site d'entreposage, au sein de l'OPA, soit pour déchets vitrifiés de type hautement radioactifs (HLW) que pour le combustible nucléaire usagé (SF), et considérant des temps égaux ou postérieurs à la vie prévue des récipients métalliques (environ 1000 ans).

En premier lieu, les flux de solutés associés aux mécanismes d'osmose chimique, d'hyperfiltration, de diffusion thermique, et d'osmose thermique ont été calculés. Ces estimations ont été obtenues à partir de données expérimentales disponibles, relatives aux processus couplés de transport dans les argiles compactées, selon les conditions hydrogéologiques et géochimiques existant dans les argiles à Opalines. Ces résultats suggèrent que seul le mécanisme couplé de l'osmose thermique peut avoir un effet important sur le transport de solutés et de fluides aux alentours du dépôt.

Dans une deuxième partie, les flux thermiques associés à la filtration thermique et à l'effet Dufour ont été calculés aux alentours du site d'entreposage. Les flux thermiques obtenus sont négligeables comparés à ceux engendrés par conduction thermique.

Lors de l'étape suivante, le but a été d'obtenir des résultats supplémentaires sur les effets de phénomènes couplés sur le transport de masse en solution. Les flux de solutés associés aux mécanismes d'advection, de diffusion chimique, d'osmose thermique et chimique, d'hyperfiltration et de diffusion thermique ont été décrits à l'aide d'une équation de transport unidimensionnelle. La solution analytique de cette équation, par le biais de paramètres appropriés, montre que l'osmose thermique est le seul processus de transport susceptible d'avoir un effet marqué sur les performances du dépôt. Ce résultat est en accord avec les estimations précédentes.

Finalement, les résultats de modèles d'écoulement simples à deux et à trois dimensions décrivant les processus d'advection (loi de Darcy) et d'osmose thermique ont montré que pour les conditions régnant au voisinage du dépôt et pour les temps d'intérêt, la composante advective de l'écoulement s'oppose à celle thermo-osmotique et l'annule.

En conclusion, l'évaluation des différents mécanismes de transport couplés a mis en évidence le très faible impact du couplage sur le transport des

radionucléides dans les argiles à Opalines, au moins pour les conditions reignant à des temps égaux ou postérieurs à la vie prévue des récipients métalliques (environs 1000 ans).

RESUM

Els fenòmens aparellats de transport (osmosi tèrmica i química, hiperfiltració, difusió aparellada, difusió tèrmica, filtració tèrmica, efecte Dufour) poden tenir un paper important en el transport de fluid, soluts i calor en formacions amb un contingut alt d'argiles, com per exemple l'Argila Opalinus (OPA). Actualment s'està plantejant la possibilitat de construir dipòsits subterranis de residus radioactius en formacions d'aquest tipus. En aquest estudi es tracten els efectes potencials de fenòmens aparellats sobre el transport de substàncies radioactives en solució prop d'un dipòsit subterrani de residus radioactius d'alt nivell vitrificats (HLW) i combustible nuclear usat (SF) situat en l'Argila Opalinus, i a escales de temps iguals o superiors a la durada prevista dels contenidors dels residus (aproximadament 1000 anys).

En primer lloc s'han estimat els fluxes de solut associats amb l'osmosi química, hiperfiltració, difusió tèrmica i osmosi tèrmica, utilitzant dades experimentals disponibles sobre argiles compactades i les condicions hidrogeològiques i geoquímiques a les que està sotmesa l'Argila Opalinus. Aquestes estimacions suggereixen que l'osmosi tèrmica és l'únic mecanisme aparellat de transport que pot tenir un efecte significatiu sobre el transport de solut i solució prop del dipòsit subterrani.

En segon lloc s'han estimat els fluxes de calor associats amb la filtració tèrmica i l'efecte Dufour prop del dipòsit subterrani. Els fluxes que s'han calculat són completament negligibles comparats amb el fluxe degut a la conducció tèrmica.

Com un pas més per entendre els efectes dels fenòmens aparellats de transport, els fluxes de solut associats amb l'advecció, difusió química, osmosi tèrmica i química, hiperfiltració i difusió tèrmica han estat incorporats en una equació simple de transport unidimensional. La solució analítica d'aquesta equació, fent servir els paràmetres adequats, indica de nou que l'osmosi tèrmica és l'únic mecanisme aparellat de transport que pot tenir un efecte important sobre el funcionament del dipòsit subterrani.

Finalment, els resultats de models simples bidimensionals i tridimensionals de fluxe de fluid que inclouen advecció (llei de Darcy) i osmosi tèrmica, mostren que sota les condicions prop del dipòsit subterrani a les escales de temps d'interès, el component advectiu del fluxe s'oposa al component d'osmosi tèrmica i l'anul·la.

Després d'avaluar els diferents mecanismes aparellats de transport, la conclusió és que aquests mecanismes només tindran un efecte molt menor sobre el transport de substàncies radioactives en l'Argila Opalinus, almenys a escales de temps iguals o superiors a la durada prevista dels contenidors dels residus (aproximadament 1000 anys).

TABLE OF CONTENTS

LIST OF FIGURES

LIST OF TABLES

1. INTRODUCTION

Coupled phenomena (thermal and chemical osmosis, hyperfiltration, coupled diffusion, thermal diffusion, thermal filtration, Dufour effect) may play an important role in fluid, solute and heat transport in clay-rich formations, such as the Opalinus Clay (OPA), which are being considered as potential hosts to radioactive waste repositories.

Rocks containing large proportions of compacted clays may act as semipermeable membranes due to the existence of ionic double layers on the clay surfaces. As surface charge on clay surfaces is usually negative, a diffuse double layer of counter-ions (cations) in solution develops right next to the mineral surface (Figure 1.1). Further details about surface charge and the formation of diffuse double layers on clays can be found in STUMM & MORGAN (1996) and HORSEMAN et al. (1996).

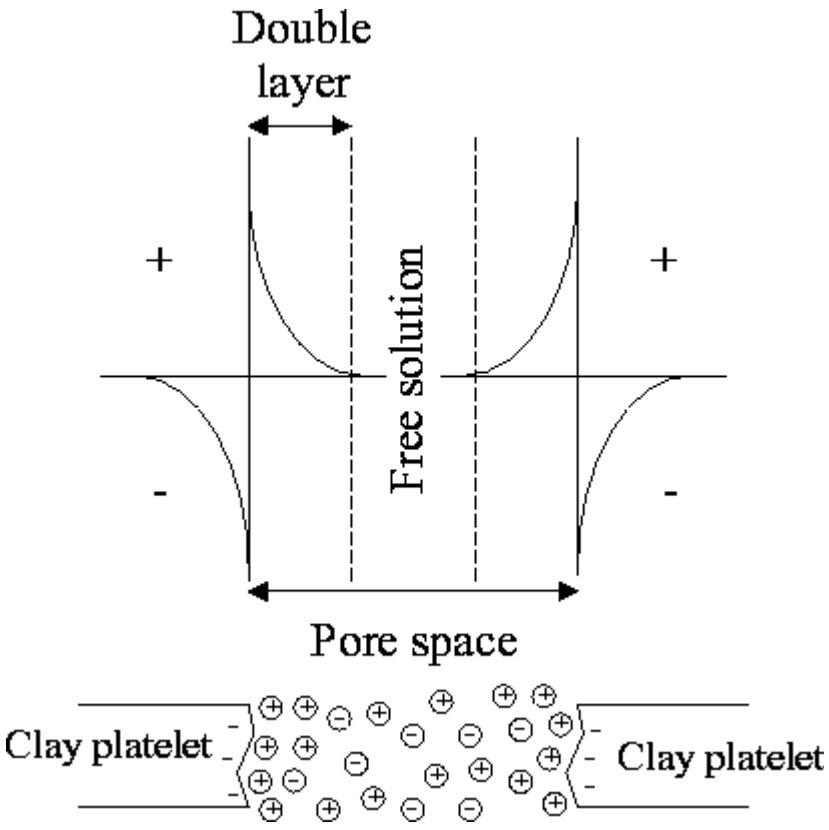

Figure 1.1: Electrical double layer in a clay pore (after MARINE & FRITZ, 1981)

If the rock is sufficiently compacted so the diffuse double layers of adjacent clay platelets overlap, the distribution of electrical charge in solution allows water and non-charged solutes to pass through the pores but prevents ionic species from doing so. Under such conditions, a clay-rich rock can potentially act as a

semipermeable membrane, with chemical osmosis, hyperfiltration, and coupled diffusion playing important roles in fluid and solute transport. Also, the existence of temperature gradients in the vicinity of a repository could promote fluid and solute transport by thermal osmosis and thermal diffusion (Soret effect). Coupled heat transport phenomena (thermal filtration, Dufour effect) could also, in principle, contribute to the heat fluxes.

The Opalinus Clay, a shale formation in northern Switzerland, has been selected as a potential host rock for a repository for vitrified high-level radioactive waste (HLW) and spent nuclear fuel (SF). An underground rock laboratory is in operation at Mont Terri, Canton Jura, Switzerland, in order to study the geological, hydrogeological, geochemical, and rock-mechanical properties of this formation. The clay mineral content of the rock ranges from 20 to 75 wt% (NAGRA, 1989a; MAZUREK, 1999), and therefore, coupled phenomena could play an active role in fluid and solute transport, including radionuclide transport, through this formation. As part of the effort to characterize the transport properties of OPA, vital to performance assessment studies of a repository, the effects of coupled phenomena have to be taken into consideration. The objective of this study is to provide estimates of the magnitudes of the fluxes associated with these coupled phenomena, and to identify the processes that may have the highest impact on performance assessment studies and possibly require further investigation.

This report is based largely on a series of PSI internal technical reports devoted to coupled transport phenomena (SOLER, 1997; SOLER 1998abc; SOLER & JAKOB, 1997).

2. DIRECT AND COUPLED TRANSPORT PHENOMENA

Coupled transport phenomena are described in the reference frame of the thermodynamics of irreversible processes. The theory of irreversible thermodynamics starts from an extension of the second law of thermodynamics, which introduces the concept of entropy (S). It can be shown that the rate of local or internal entropy production of a given system, per unit volume, can be written in terms of

$$\frac{1}{V}\frac{dS}{dt} = \sum_i \mathrm{J}_i X_i \tag{2.1}$$

where V is the volume of the system, J_i is a flux (e.g. flux of heat, fluid, solutes, electrical current), and the X_i terms are driving forces (e.g. temperature, hydraulic, chemical potential, or electrical potential gradients). The assumption in the theory of irreversible thermodynamics is that the forces appearing in Eqn. 2.1 are the only forces needed to fully describe the kinetics and evolution of the system (Lasaga, 1998). If this assumptions holds, the second law of thermodynamics will state that

$$\sum_i \mathrm{J}_i X_i \geq 0 \tag{2.2}$$

which means that each flux term is a function (although unknown) of all the driving forces. Now, an additional assumption is that this function is linear, and therefore, a flux can be expressed as

$$\mathrm{J}_i = \sum_j L_{ij} X_j \tag{2.3}$$

where the L_{ij} terms are the so-called phenomenological coefficients. The term direct or diagonal phenomena is used for the $L_{ii} X_i$ contribution to a flux J_i, and the term coupled or off-diagonal phenomena is used for the $L_{ij} X_j$ contribution when $j \neq i$. Also, the phenomenological coefficients associated with coupled phenomena are related by the Onsager Reciprocal Relations (ONSAGER, 1931)

$$L_{ij} = L_{ji} \tag{2.4}$$

Table 2.1 is the matrix for direct and coupled phenomena for different transport processes. In this study, the effects of thermal, hydraulic, and chemical gradients, on heat, fluid, and solute fluxes, will be considered. The effects of possible natural electric potential gradients on the different fluxes have not been considered in this study. To date, there is no information regarding electric potential gradients in the Opalinus Clay, and although it is true that

spontaneous potentials are measured in clay formations, it is not clear what the connection is between a potential at a microscopic scale (surface charge on clays, formation of diffuse double layers), which may be the cause of such spontaneous potentials, and one at a macroscopic (metric) scale. Also, only very scarce information is available regarding the coupling coefficients for coupled transport phenomena driven by electric potential gradients.

Table 2.1: Onsager matrix - Matrix of direct (diagonal) and coupled (off-diagonal) transport phenomena (DE MARSILY, 1986; HORSEMAN et al., 1996). Shaded boxes correspond to the processes considered in this study

	POTENTIAL GRADIENT X			
FLUX J	**Temperature**	**Hydraulic**	**Chemical**	**Electrical**
Heat	Thermal conduction	Thermal filtration	Dufour effect	Peltier effect
Fluid	Thermal osmosis	Advection	Chemical osmosis	Electrical osmosis
Solute	Thermal diffus. or Soret effect	Hyperfiltration	Diffusion	Electro-phoresis
Current	Seebeck or Thompson eff.	Rouss effect	Diffusion & Membr. Pot.	Electrical conduction

Given a system composed of water and n species in solution, and following the formulations used by CARNAHAN (1984), DE GROOT & MAZUR (1962), and KATCHALSKY & CURRAN (1965), the fluxes of heat (J_q^0), fluid (J_v), and solute (J_i^0), per unit total (rock) cross-section area, are given by

Heat flux:
$$J_q^0 = -L_{qq}\frac{\nabla T}{T^2} - L_{qv}\nabla\left(\frac{h'}{T}\right) - \sum_{k=1}^{n} L_{qk}\frac{\nabla\left(\mu_k / T\right)}{W_k} \qquad (2.5)$$

Fluid flux:
$$J_v = -L_{vq}\frac{\nabla T}{T^2} - L_{vv}\nabla\left(\frac{h'}{T}\right) - \sum_{k=1}^{n} L_{vk}\frac{\nabla\left(\mu_k / T\right)}{W_k} \qquad (2.6)$$

Solute flux: $$J_i^0 = -L_{iq}\frac{\nabla T}{T^2} - L_{iv}\nabla\left(\frac{h'}{T}\right) - \sum_{k=1}^{n} L_{ik}\frac{\nabla\left(\mu_k / T\right)}{W_k} \qquad i = 1,\ldots,n \qquad (2.7)$$

where the driving forces are the temperature gradient (∇T), hydraulic gradient ($\nabla h' = \nabla p + \rho g \nabla z$), and the concentration- and temperature-dependent part of the chemical potential gradient ($\nabla \mu_k$). The chemical potential μ_k has units of J/mol. P is the fluid pressure, ρ is the fluid density, ϕ is porosity, and W_k is the molar weight of species k. The three terms on the right-hand-side of Eqn. 2.5 correspond to thermal conduction, thermal filtration, and the Dufour effect, respectively. The terms on the right-hand-side of Eqn. 2.6 correspond to thermal osmosis, advection, and chemical osmosis, and the three terms on the right-hand-side of Eqn. 2.7 correspond to thermal diffusion, hyperfiltration, and chemical diffusion. All the parameters are defined in the list of symbols, at the end of the report.

In this formulation, which is valid for a system at mechanical equilibrium (approximately constant fluid velocity; KATCHALSKY & CURRAN, 1965), J_i^0 refers to the flux of solute inside a fluid packet, i.e., subtracting any component caused by fluid flow. The total solute flux for a species i will be given by

$$J_i = J_i^0 + c_i J_v \qquad (2.8)$$

where c_i is the mass concentration (kg/m^3) of solute i, and J_v is the flux of fluid (solution), in units of cubic meter of fluid per square meter of rock per second. Notice that for each fluid transport mechanism (thermal osmosis, advection, chemical osmosis) there is an associated flux of solute, arising from the second term on the right-hand-side of Eqn. 2.8. The same kind of relationship applies also to heat transport (there is a heat flux component associated with each fluid transport mechanism). The total heat flux will be given by

$$J_q = J_q^0 + \rho c_f T J_v \qquad (2.9)$$

where ρ (kg/m^3) and c_f (J/kg/K) are the density and heat capacity of the fluid, respectively.

It is also possible to use a somewhat simpler formulation, especially if one wants to look only at fluid and solute transport. Making use of

$$\nabla\left(\frac{\mu_k}{T}\right) = \frac{1}{T}\nabla\mu_k - \frac{\mu_k}{T^2}\nabla T \qquad (2.10)$$

and

$$\nabla\left(\frac{h'}{T}\right)=\frac{1}{T}\nabla h'-\frac{h'}{T^2}\nabla T \tag{2.11}$$

and using

$$T\frac{1}{V}\frac{dS}{dt}=\sum_i \mathrm{J}_i X_i \tag{2.12}$$

instead of Eqn. 2.1, Eqns. 2.5, 2.6, and 2.7 can be rewritten as

$$J_s=-L'_{qq}\nabla T-L'_{qv}\nabla h'-\sum_{k=1}^{n}L'_{qk}\nabla\left(\frac{\mu_k}{W_k}\right) \tag{2.13}$$

$$J_v=-L'_{vq}\nabla T-L'_{vv}\nabla h'-\sum_{k=1}^{n}L'_{vk}\nabla\left(\frac{\mu_k}{W_k}\right) \tag{2.14}$$

$$J_i^0=-L'_{iq}\nabla T-L'_{iv}\nabla h'-\sum_{k=1}^{n}L'_{ik}\nabla\left(\frac{\mu_k}{W_k}\right)\qquad i=1,\ldots,n \tag{2.15}$$

where J_s (J/K/m^2/s) is the flux of entropy driven by a temperature gradient, defined as

$$J_s=\frac{J_q^0-\sum_{i=1}^{n}J_i^0\frac{\mu_i}{W_i}-J_v h'}{T} \tag{2.16}$$

3. ESTIMATES OF SOLUTE FLUXES ASSOCIATED WITH COUPLED TRANSPORT PHENOMENA

In this section, the effects of hydraulic, temperature, and chemical gradients, on solute and fluid (solution) transport will be estimated, using the hydrogeological and geochemical conditions at the Mont Terri Reconnaisance Tunnel (host of the Mont Terri rock laboratory for the Opalinus Clay) and other drilling locations in northern Switzerland as reference for the calculations. The transport processes that will be considered are advection, thermal osmosis, chemical osmosis, hyperfiltration, thermal diffusion, and chemical diffusion. All solute fluxes associated with direct and coupled phenomena will not be written in terms of strict irreversible thermodynamics, subject to the Onsager Reciprocal Relations, but in terms of parameters and gradients that are commonly measured in field or laboratory experiments. The advective and diffusive solute fluxes will be used as the references to which the other fluxes will be compared.

3.1 Formulation of the solute fluxes

The different solute fluxes, all of them in units of kg/m^{2}rock/s, are formulated as follows:

Advection $$J_{ADV} = -c_i K \frac{\partial h}{\partial x} \quad (3.1)$$

Chemical diffusion $$J_D = -D_e \frac{\partial c_i}{\partial x} \quad (3.2)$$

Chemical osmosis $$J_{CO} = c_i \sigma K \frac{\partial \Pi_h}{\partial x} \quad (3.3)$$

Hyperfiltration $$J_{HYP} = c_i \sigma K \frac{\partial h}{\partial x} \quad (3.4)$$

Thermal diffusion $$J_{TD} = -D_e s c_i \frac{\partial T}{\partial x} \quad (3.5)$$

Thermal osmosis $$J_{TO} = -c_i k_T \frac{\partial T}{\partial x} \quad (3.6)$$

A detailed explanation of the formulation used for the fluxes is given below (all parameters are also defined in the list of symbols).

3.1.1 Advection

Here, the flux of fluid associated with advection (Darcy velocity, v_D), in units of volume of fluid per unit cross-section area of rock per unit time, will be written according to Darcy's law, expressed in terms of hydraulic conductivities and hydraulic heads. In one dimension, Darcy's law has the form

$$v_D = -K\frac{\partial h}{\partial x} \tag{3.7}$$

The hydraulic conductivity (K) is related to the phenomenological coefficient for advection (L'_{vv}) by the equation

$$K = \rho g L'_{vv} \tag{3.8}$$

where ρ is the density of the fluid, and g is the gravitational acceleration.

The solute flux associated with advection is given by Eqn. 3.1.

3.1.2 Chemical diffusion

The diffusive solute flux will be written in terms of Fick's first law, given by Eqn. 3.2. D_e is the effective diffusion coefficient for species i, which can be given in terms of (a)

$$D_e = \phi\left(\frac{\chi}{\tau^2}\right)D_0 \tag{3.9}$$

where χ and τ are the constrictivity and tortuosity of the porous medium, respectively, and D_0 is the molecular diffusion coefficient of species i in water, or (b)

$$D_e = \frac{D_0}{F} \tag{3.10}$$

where F (the resistivity or formation factor) is given by

$$F = \phi^{-m} \tag{3.11}$$

and m (the cementation exponent) has reported values between 1.3 and 5.4 (HORSEMAN et al., 1996, and references within), and values around 2 for deeply buried compacted sediments (ULLMAN & ALLER, 1982).

Coupled diffusion (the diffusive flux of one species driven by the chemical potential gradients of other species) will not be considered when estimating the solute fluxes associated with the different transport mechanisms. The goal is to

compare the solute fluxes associated with coupled phenomena to the diffusive flux as given by Eqn. 3.2 and see what the additional effect is.

In the case of simple (binary) aqueous electrolyte solutions, coupled diffusion has been shown to be due to the coulombic coupling between cation and anion. When cation and anion have different intrinsic (tracer) diffusion coefficients, the value of the net combined interdiffusion coefficient falls in between the values of the two individual tracer diffusion coefficients (LASAGA, 1998). In the case of a clay-rich rock with overlapping double layers, the negative charge on the surface of the clays will prevent (to some extent) anions from passing through the pores. This phenomenon, known as anion exclusion, will in turn cause a reduction of the cation flux, because of coulombic coupling (charge balance).

The relationship between the effective diffusion coefficient D_e and the diffusive flux written in terms of irreversible thermodynamics (last term of Eqn. 2.7), ignoring coupled diffusion, is given by

$$D_e = \frac{L'_{ii}}{W_i}\frac{\partial \mu_i}{\partial c_i} \tag{3.12}$$

where L_{ii} is the phenomenological coefficient for direct diffusion (diffusion of a species driven by the chemical potential gradient of the same species), and W_i and μ_i are the molar weight (kg/mol) and chemical potential (J/mol) of species i.

3.1.3 Chemical osmosis

Chemical osmosis is the flow of fluid (solution) caused by chemical potential gradients. Chemical-osmotic flow across a semipermeable membrane is up the salinity gradient, or equivalently, down the activity of water gradient.

The chemical-osmotic flux of fluid is given in the last term of Eqn. 2.6 or 2.14, but can also be expressed in terms of a flow law similar to Darcy's law (KEMPER & EVANS, 1963; KEMPER & ROLLINS, 1966; BARBOUR & FREDLUND, 1989). This flow law, in one dimension, and with units of m^3/m^2rock/s, has the form

$$v_{CO} = K_\pi \frac{\partial \Pi_h}{\partial x} = \sigma K \frac{\partial \Pi_h}{\partial x} \tag{3.13}$$

where K_π is the coefficient of osmotic permeability, σ is the coefficient of osmotic efficiency ($0 \le \sigma \le 1$), K is the hydraulic conductivity, and Π_h is the osmotic pressure head.

The coefficient of osmotic efficiency (σ) is a measure of how close to ideal a semipermeable membrane is. For an ideal membrane (no solute flux through

the membrane is allowed) σ is equal to one. On the other hand, if there is no restriction on the flux of solute through the membrane, σ is equal to zero.

The osmotic pressure head, Π_h, is defined as

$$\Pi_h = \frac{\Pi}{\rho g} \tag{3.14}$$

and the osmotic pressure, Π, is given by

$$\Pi = -\frac{RT}{V_w} \ln a_w \tag{3.15}$$

where V_w and a_w are the molar volume and activity of water, respectively. The activity of water can be calculated according to (GARRELS & CHRIST, 1965)

$$a_w = 1 - V_w \sum_i \frac{c_i}{W_i} \tag{3.16}$$

Equation 3.3 describes, in one dimension, the solute flux associated with chemical osmosis.

3.1.4 Hyperfiltration

Hyperfiltration is the flow of solutes up the hydraulic gradient, caused by the fact that an ideal semipermeable membrane will let water flow by advection through the pores but will prevent solutes from doing so. The hyperfiltration flux can be written as in Eqn. 3.4 (GROENEVELT, ELRICK & LARYEA, 1980) where σ, again, is the coefficient of osmotic efficiency. In reality, this coefficient has a specific value for each different species (just like the hyperfiltration phenomenological coefficient L_{iv}; see Eqn. 2.7). However, for the estimates presented in this study, the same average value of σ as in the formulation of the chemical-osmotic flux (Eqn. 3.3) will be used (this would only be strictly true for the case of a solution of a single salt, e.g. a NaCl solution).

3.1.5 Thermal diffusion

Thermal diffusion promotes the transport of solutes due to temperature gradients. The solute flux caused by thermal diffusion is given in the first term on the right-hand-side of Eqn. 2.7. However, thermal diffusion coefficients are usually reported in the literature as Soret coefficients (s), which arise from a formulation of thermal diffusion according to Eqn. 3.5. Soret coefficients measured in the laboratory are usually positive, i.e., they indicate solute transport down temperature gradients, and range between 10^{-3} and 10^{-2} K^{-1},

under a whole range of concentrations and temperatures (LERMAN, 1979; THORNTON & SEYFRIED, 1983; DE MARSILY, FARGUE & GOBLET, 1987).

3.1.6 Thermal osmosis

Thermal osmosis causes the flow of fluid (solution) down a temperature gradient. The flux of fluid caused by thermal osmosis is given in the first term on the right-hand-side of Eqn. 2.6 or 2.14, but it has also been written as (DIRKSEN, 1969)

$$v_{TO} = -k_T \frac{\partial T}{\partial x} \tag{3.17}$$

where k_T is the thermo-osmotic permeability ($m^2/K/s$) of the medium. v_{TO} has units of m^3/m^2rock/s. The solute flux associated with thermal osmosis is given by Eqn. 3.6.

3.2 Diffusion coefficients and hydraulic conductivities for the Opalinus Clay

Since the solute fluxes associated with coupled transport phenomena will be estimated by means of comparing them to advective and chemical-diffusive fluxes, it is necessary, first of all, to establish the basic transport properties of the Opalinus Clay, namely hydraulic conductivities (K) and effective diffusion coefficients (D_e).

3.2.1 Hydraulic conductivities

Field tests have indicated that hydraulic conductivities for the Opalinus Clay (OPA) are less than 10^{-11} m/s (NAGRA, 1989a). Also, laboratory measurements (HARRINGTON & HORSEMAN, 1999; DE WINDT & PALUT, 1999) have yielded values between 10^{-14} and $8 \cdot 10^{-14}$ m/s. Based on these measurements, the chosen range of values for the hydraulic conductivity of OPA goes from 10^{-14} to 10^{-12} m/s, with an extended range (less probable values) reaching up to 10^{-11} m/s.

$$K\text{: } 10^{-14} \cdots 10^{-12}\ (10^{-11})\ \mathrm{m/s}$$

3.2.2 Diffusion coefficients

Porosity values for OPA determined from weight loss measurements due to evaporation of pore water range from 12% to 19% (MAZUREK, 1999). Porosities determined from Hg injection porosimetry and Cl content, which reflect geochemical or diffusion-accessible porosities, range from 5% to 11%

(MAZUREK, 1999). Based on these values, relatively low temperatures (25 - 60 °C), and assuming that the effective diffusion coefficient for OPA can be calculated according to

$$D_e = \phi^m D_0 \tag{3.18}$$

with a value of m around 2 (ULLMAN & ALLER, 1982), and D_0 =10^{-9} m^2/s at 25°C (see for instance LI & GREGORY, 1974), the range for effective diffusion coefficients goes from 10^{-12} to 10^{-11} m^2/s, with an extended range (less probable values) going from 10^{-13} to 10^{-10} m^2/s.

$$D_e: 10^{-12} \cdots 10^{-11}\ (10^{-13} \cdots 10^{-10})\ \mathrm{m}^2/\mathrm{s}$$

Laboratory measurements of effective diffusion coefficients for tritiated water and iodine in Opalinus Clay samples have provided values in that same range from 10^{-12} to 10^{-11} m^2/s (DE WINDT & PALUT, 1999).

3.2.3 K/D_e

The ratio K/D_e, which will be used in the following sections, ranges from 10^{-3} to 1 m^{-1}, or from 10^{-4} to 100 m^{-1} in the extended range.

$$K/D_e: 10^{-3} \cdots 1\ (10^{-4} \cdots 100)\ \mathrm{m}^{-1}$$

3.3 Chemical diffusion vs. advection

As it has already been mentioned, the solute fluxes associated with coupled phenomena will be compared to both diffusive and advective fluxes. Therefore, in order to have the means to estimate the relative importance of all the different transport mechanisms, it will be necessary to compare first the magnitudes of chemical diffusion and advection. Advective and diffusive fluxes will be compared by means of (a) Peclet numbers, and (b) assuming values for concentration gradients. This last method will be later used to compare the solute fluxes associated with coupled phenomena to diffusive fluxes.

3.3.1 Peclet number

The dimensionless Peclet number is defined here as

$$Pe = \frac{v_D L}{D_e} \tag{3.19}$$

or equivalently

$$Pe = \frac{\left| K \frac{\partial h}{\partial x} \right| L}{D_e} = \frac{K}{D_e} \left| \frac{\partial h}{\partial x} \right| L \qquad (3.20)$$

where v_D is the Darcy velocity (its magnitude in this case), h is the hydraulic head, and L is an arbitrary reference length or distance. At a spatial scale defined by this reference length L, advection will be dominant over chemical diffusion if $Pe >> 1$, and chemical diffusion will be dominant if $Pe << 1$.

Assuming $\left| \partial h / \partial x \right| = 1$, a reasonable value given the measured hydraulic heads in OPA and the aquifers above and below (NAGRA, 1994), and given the range of values for K/D_e (see section 3.2.3), the range of values for Pe is

$$Pe\text{: } 10^{-3} \times \mathrm{L} \cdots 1 \times L \ \ (10^{-4} \times L \cdots 100 \times L)$$

where the values in parentheses correspond to the extended (less probable) range for K/D_e. The reference length L corresponding to $Pe = 1$ ($L_{Pe=1}$), is an indication of the length scale at which advective and diffusive transport are approximately of the same magnitude. The range of values for $L_{Pe=1}$ is

$$L_{Pe=1}\text{: } 1000 \cdots 1 \text{ m} \ \ (10^{4} \cdots 10^{-2} \text{ m})$$

For spatial dimensions less than $L_{Pe=1}$ diffusion will be dominant with respect to advection. The large values for $L_{Pe=1}$ show that diffusion will be more important than advection in most cases. Also, if the hydraulic gradient were smaller than unity, diffusion would even be more dominant.

3.3.2 Assume values for concentration gradients

Taking the conditions at Mt. Terri as reference (Fig. 3.1), with high salinities in OPA and low salinities outside OPA, one can imagine the concentration of a given species i in solution as going from a value of c_i in OPA to a much smaller value (namely zero) outside OPA. The data in Fig. 3.1 show that change occurring at the most in a distance of about 100 m (perpendicular to bedding), although it may be that the gradient is steeper close to the boundary of the formation. If such change in concentration occurred in a distance of 100, 10, or 1 m, the resulting average concentration gradient would be $c_i/100$, $c_i/10$, or $c_i/1$ kg/m^3/m, respectively. With these values of the concentration gradients it is now possible to calculate the diffusive fluxes (Eqn. 3.2), which will give the diffusive flux (J_D) as a function of c_i. Having done this, concentrations (c_i) can be expressed as functions of the diffusive fluxes:

$$\frac{\Delta c_i}{\Delta x} = c_i/1m \Rightarrow J_D = -D_e c_i \Rightarrow c_i = \left|J_D/D_e\right|$$

$$\frac{\Delta c_i}{\Delta x} = c_i/10m \Rightarrow J_D = -10^{-1} D_e c_i \Rightarrow c_i = 10\left|J_D/D_e\right|$$

$$\frac{\Delta c_i}{\Delta x} = c_i/100m \Rightarrow J_D = -10^{-2} D_e c_i \Rightarrow c_i = 100\left|J_D/D_e\right|$$

The three different expressions correspond to the three different concentration gradients.

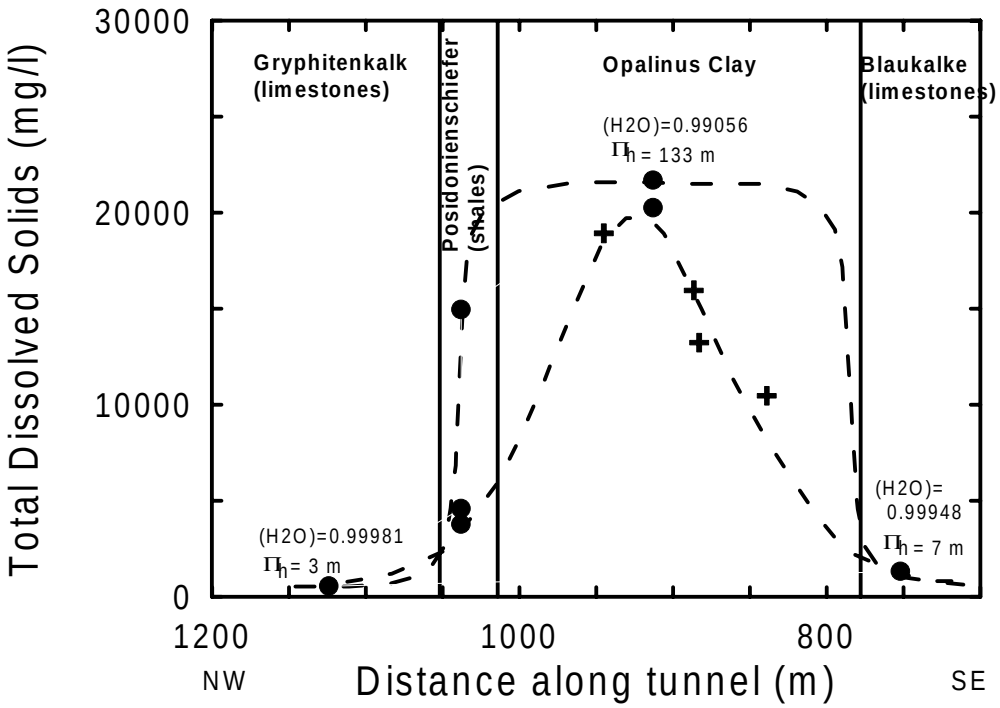

Figure 3.1: Schematic diagram showing Total Dissolved Solids vs. Distance along the Mt. Terri tunnel. TDS data from GAUTSCHI, ROSS & SCHOLTIS, 1993 (solid circles), and PEARSON et al., 1999 (crosses). Activity of water (H_2O) and osmotic pressure head (Π_h) are also given for the sample with the highest salinity in OPA, and for two low-salinity samples above and below OPA. The dashed lines are hypothetical salinity curves. The vertical lines are only intended to show the boundaries of the different rock units along the tunnel. The orientation of the tunnel is NW-SE, and the rock strata dip at an angle of about 45° to the southeast. The thickness of the Opalinus Clay at the Mont Terri tunnel is about 140 m (THURY, 1997).

If the expression for the advective flux J_{ADV} (Eqn. 3.1) is now recalled, and assuming a unit hydraulic gradient ($\partial h / \partial x = 1$), J_{ADV} will be given, in absolute value, and from large to small concentration gradients, by

$$\left|J_{ADV}\right| = Kc_i = K\left|J_D / D_e\right| \tag{3.21}$$

$$\left|J_{ADV}\right| = Kc_i = 10K\left|J_D / D_e\right| \tag{3.22}$$

$$\left|J_{ADV}\right| = Kc_i = 100K\left|J_D / D_e\right| \tag{3.23}$$

Using these expressions and the values of K/D_e from section 3.2.3, the range of values for the ratio $\left|J_{ADV} / J_D\right|$ is

$$\left|J_{ADV} / J_D\right|: 10^{-3} \cdots 100 \ \ (10^{-4} \cdots 10^{4})$$

These values indicate that either diffusion or advection could be, in principle, dominant. However, if hydraulic gradients were less than unity, diffusion would tend to become more clearly the dominant transport mechanism. Also, if the concentration gradients were relatively steep, the lower values of $\left|J_{ADV} / J_D\right|$ would apply.

3.4 Hyperfiltration

Since hyperfiltration promotes the transport of solute up the hydraulic gradient (see Eqn. 3.4), it will always tend to oppose to advection, and it can only be as large in magnitude as advection ($\left|J_{HYP}\right| = \left|J_{ADV}\right|$ if $\sigma = 1$). Also, any hyperfiltration flux would be in principle beneficial for repository performance (it would act against advective release of radionuclides from a rock hosting a nuclear waste repository).

3.5 Chemical osmosis

Chemical osmosis is the flow of fluid (solution) caused by chemical potential gradients. Chemical osmotic flow across a semipermeable membrane is up the salinity gradient (down activity of water gradient). The chemical osmotic flux of fluid, and the solute flux associated with it, are described here in terms of a flow law similar to Darcy's law (Eqn. 3.3).

3.5.1 Chemical osmosis vs. advection

The chemical-osmotic and advective fluxes are given by Eqns. 3.3 and 3.1, and the ratio between the two fluxes is given by

$$\left|\frac{J_{CO}}{J_{ADV}}\right| = \left|\frac{\sigma \frac{\partial \Pi_h}{\partial x}}{\frac{\partial h}{\partial x}}\right| \qquad (3.24)$$

The first measurements of osmotic efficiencies of OPA samples in the laboratory (HARRINGTON & HORSEMAN, 1999) give values of σ around 0.1. And in order to estimate the osmotic pressure head gradient, the same approach used for the concentration gradients will be applied. Looking again at the situation at Mt. Terri (Fig. 3.1), it can be seen that the magnitude of the change in osmotic pressure head is about 100 m, and occurs at the most in a distance of about 100 m (that distance could also be smaller). If that change happens in 100, 10, or 1 m, $\partial \Pi_h / \partial x$ will be 1, 10, or 100, respectively. With this range of values for the osmotic pressure head gradient, and assuming again a unit hydraulic gradient, a range of values for $\left|J_{CO}/J_{ADV}\right|$ can be obtained:

$$\left|J_{CO}/J_{ADV}\right|: 0.1 \cdots 10$$

This estimate seems to indicate that, under conditions similar to the ones prevailing at Mt. Terri, advective and chemical osmotic fluxes will be similar in magnitude. Chemical osmotic fluxes could only be significantly larger than advective fluxes if hydraulic gradients were smaller than unity.

3.5.2 Chemical osmosis vs. chemical diffusion

Assuming that both concentration and osmotic pressure head (which is related to the activity of water and salinity) vanish in about the same distance, i.e., they go from their values inside OPA to very small values outside in about the same distance, the chemical osmotic flux will be given by

$$J_{CO} = c_i \sigma K \frac{\partial \Pi_h}{\partial x} = 10 K \left|\frac{J_D}{D_e}\right| \qquad (3.25)$$

where c_i has again been given as a function of the diffusive flux, and a value of σ equal to 0.1 has been assumed. Given the values for K/D_e (see section 3.2.3), the range of values for the ratio between chemical-osmotic and diffusive fluxes is

$$\left|J_{CO}/J_D\right|: 10^{-2} \cdots 10 \ \ (10^{-3} \cdots 10^{3})$$

Again, it looks like only under some conditions (relatively high K/D_e ratios) could the chemical osmotic flux be larger in magnitude than the diffusive flux.

Also, the fact that chemical osmosis promotes the flow of fluid up the salinity gradient, means that for conditions similar to the ones at Mt. Terri (Fig. 3.1), any chemical osmotic flux would be directed towards OPA (up the salinity gradient). Therefore, in principle, any contribution to the total flux from chemical osmosis would be beneficial for the performance of the repository (against the release of radionuclides from OPA).

3.6 Thermal diffusion

Thermal diffusion promotes the transport of solutes due to temperature gradients, and is formulated according to Eqn. 3.5.

3.6.1 Thermal diffusion vs. advection

Thermal-diffusive and advective fluxes are given by Eqns. 3.5 and 3.1. Assuming a unit hydraulic gradient, the temperature gradient at which both fluxes are equal in magnitude is

$$\left|\frac{\partial T}{\partial x}\right|_{eq} = \frac{K}{D_e s} \tag{3.26}$$

Table 3.1 shows values of this temperature gradient for different values of the Soret coefficient, and making use of the assumed range of values for K/D_e .

Table 3.1: Table of temperature gradients at which $|J_{TD}| = |J_{ADV}|$. Values in parentheses correspond to the extended (less probable) range for K/D_e .

s (K^{-1})	$\left\|\partial T/\partial x\right\|_{eq}$ (K/m)
10^{-3}	1 – 1000 (0.1 – 10^5)
$5x10^{-3}$	0.2 – 200 (0.02 – $2x10^4$)
10^{-2}	0.1 – 100 (0.01 – 10^4)
$2x10^{-2}$	0.05 – 50 (0.005 – $5x10^3$)

Model calculations (SATO et al., 1998) suggest that temperature gradients near the repository at the time of waste canister failure ($t \approx 1000$ y) will be less than 1 K/m, and probably only about 0.25 K/m. Values of $\left|\partial T/\partial x\right|_{eq}$ in Table 3.1 are

only less than 0.25 K/m, and even less than 1 K/m, for the lowest values of K/D_e (temperature gradients larger than those in the table would mean that thermal diffusion would be more important than advection). It seems thus very probable that thermal diffusive fluxes will be smaller than advective fluxes.

3.6.2 Thermal diffusion vs. chemical diffusion

Thermal-diffusive and chemical-diffusive fluxes are given by Eqns. 3.5 and 3.2. The temperature gradient at which both fluxes are equal in magnitude is

$$\left|\frac{\partial T}{\partial x}\right|_{eq} = \frac{\left|\partial c_i / \partial x\right|}{s c_i} \tag{3.27}$$

Table 3.2 shows values of this temperature gradient for different Soret coefficients and concentration gradients.

Table 3.2: $\left|\partial T/\partial x\right|_{eq}$ in K/m, as a function of Soret coefficients (K^{-1}) and concentration gradients ($kg/m^3/m$).

	s (K^{-1})			
$\Delta c_i/\Delta X$ (kg/m^4)	**0.001**	**0.005**	**0.01**	**0.02**
$c_i/1$	1000	200	100	50
$c_i/10$	100	20	10	5
$c_i/100$	10	2	1	0.5

No temperature gradients less than 0.25 K/m are obtained for the selected values of the concentration gradients and Soret coefficients. And gradients less than 1 K/m are only obtained for Soret coefficients larger than 0.01 K^{-1} and the smallest concentration gradients. Again, these estimates suggest that chemical diffusion will be more important than thermal diffusion.

3.7 Thermal osmosis

A big source of uncertainty in evaluating the potential role of thermal osmosis is the lack of data regarding the thermo-osmotic permeability k_T. Reported values of k_T for Na-saturated kaolinite and Na-bentonite (DIRKSEN, 1969), at an

average temperature of 25 °C and various temperature gradients and porosities, range between 10^{-14} and $3x10^{-13}$ $m^2/K/s$. In another study (SRIVASTAVA & AVASTHI, 1975) thermal osmosis across a kaolinite membrane was investigated. An estimate of k_T from the data in SRIVASTAVA & AVASTHI (1975), corresponding to conditions similar to the ones giving the high k_T values in DIRKSEN (1969), yields a value of $2.6x10^{-10}$ $m^2/K/s$, which is three orders of magnitude larger !

As a first approximation, the values of k_T mentioned above can be used to define a range of values:

$$k_T: 10^{-14} \cdots 10^{-10} \ \mathrm{m^2 / K / s}$$

3.7.1 Thermal osmosis vs. advection

The thermal-osmotic and advective solute fluxes are given by Eqns. 3.6 and 3.1. Assuming a unit hydraulic gradient, the temperature gradient at which both fluxes are equal in magnitude is given by

$$\left|\frac{\partial T}{\partial x}\right|_{eq} = \frac{K}{k_T} \tag{3.28}$$

If a value of k_T equal to 10^{-10} $m^2/K/s$ (worst case) is used to estimate this temperature gradient, and with the hydraulic conductivities (K) described in section 3.2.1, the following range of values is obtained:

$$\left|\frac{\partial T}{\partial x}\right|_{eq} = 10^{-4} \cdots 10^{-2} \ (10^{-1}) \ \mathrm{K / m}$$

where the number in parentheses corresponds to K=10^{-11} m/s.

These are very small temperature gradients (smaller than the 0.25 K/m discussed in section 3.6.1), and suggest that thermal osmosis could have a significant effect (the thermal osmotic flux will be larger in magnitude than the advective flux if the temperature gradient is larger than $\left|\partial T/\partial x\right|_{eq}$).

It should be mentioned, however, that the smallest K/k_T ratio measured on the same sample, which defines $\left|\partial T/\partial x\right|_{eq}$, gives only a value of about 2 K/m (SRIVASTAVA & AVASTHI, 1975). This value would mean that unless hydraulic gradients were significantly smaller than unity, the thermal osmotic flux would be smaller in magnitude than the advective flux.

3.7.2 Thermal osmosis vs. chemical diffusion

Using the approach previously described of expressing concentrations as functions of the diffusive fluxes, the thermal osmotic flux (Eqn. 3.6) can be formulated, from large (c_i /1) to small (c_i /100) concentration gradients, as

$$\left|J_{TO}\right| = \left|\frac{J_D}{D_e} k_T \frac{\partial T}{\partial x}\right| \tag{3.29}$$

$$\left|J_{TO}\right| = 10\left|\frac{J_D}{D_e} k_T \frac{\partial T}{\partial x}\right| \tag{3.30}$$

$$\left|J_{TO}\right| = 100\left|\frac{J_D}{D_e} k_T \frac{\partial T}{\partial x}\right| \tag{3.31}$$

Using the expression of $\left|J_{TO}\right|$ for the largest concentration gradient (Eqn. 3.29), which corresponds to the most favorable case for diffusion, the temperature gradient corresponding to equal thermal-osmotic and diffusive fluxes is given by

$$\left|\frac{\partial T}{\partial x}\right|_{eq} = \frac{D_e}{k_T} \tag{3.32}$$

Using again k_T =10^{-10} m^2/K/s and the values for D_e given in section 3.2.2, the possible range of values for $\left|\partial T/\partial x\right|_{eq}$ is

$$\left|\frac{\partial T}{\partial x}\right|_{eq} = 10^{-2} \cdots 10^{-1} \ \ (10^{-3} \cdots 1) \ \text{K/m}$$

with the values in parentheses corresponding to the extended range of values for D_e. Again, these are very small gradients, suggesting that thermal osmotic fluxes could be much larger than diffusive fluxes.

Summarizing, thermal osmosis could have a very strong impact on both solute and fluid transport in the vicinity of a radioactive waste repository hosted by the Opalinus Clay if the larger values for the thermo-osmotic permeability apply. Thermal osmosis promotes solute and fluid transport down the temperature gradient, and should, in principle, be of concern in the design of the repository.

4. ESTIMATES OF THE HEAT FLUXES ASSOCIATED WITH THERMAL FILTRATION AND THE DUFOUR EFFECT

4.1 Thermal filtration

Thermal filtration is the flux of heat caused by hydraulic gradients. Due to the lack of experimental observations, the Onsager Reciprocal Relations (ORR) will be used to obtain values for the phenomenological coefficient associated with thermal filtration (L_{qv}).

The thermal-osmotic flux of fluid (solution) per total cross-section area, which is the flux of fluid caused by a temperature gradient, is given by Eqn. 3.17. Equivalently, the same flux can be expressed, according to irreversible thermodynamics (see Eqn. 2.6), as

$$v_{TO} = -L_{vq} \frac{\nabla T}{T^2} \tag{4.1}$$

Combining Eqns. 3.17 and 4.1, and making also use of the Onsager Reciprocal Relations $(L_{qv} = L_{vq})$, an expression for the phenomenological coefficient for thermal filtration is obtained. This expression has the form

$$L_{qv} = k_T T^2 \tag{4.2}$$

Now, the heat flux caused by thermal filtration, in units of energy per unit total cross-section area per time is given by

$$J_{TF} = -L_{qv} \nabla\left(\frac{h'}{T}\right) \tag{4.3}$$

If the temperature gradient is sufficiently small, which is the case for the time scales considered here (t $\geq$ 1000 y), it may be a good approximation to take the temperature term outside the derivative and rewrite Eqn. 4.3 as

$$J_{TF} = -L_{qv} \frac{1}{T} \nabla h' \tag{4.4}$$

Combining Eqns. 4.2 and 4.4, and expressing the hydraulic gradient in terms of hydraulic head $(h = P/\rho g + z)$, the flux can be written as

$$J_{TF} = -k_T T \rho g \nabla h \tag{4.5}$$

where ρ is the fluid density and g is the gravitational acceleration. An estimate of the heat flux associated with thermal filtration can be calculated if the parameters in Eqn. 4.5 are chosen so they are representative of the conditions

in the vicinity of a repository for vitrified high level waste and spent fuel hosted by the Opalinus Clay at the time of waste canister failure ($t \approx 1000$ y). The values that have been used are:

k_T: $10^{-14} \cdots 10^{-10}$ $m^2 / K / s$ (range of experimental measurements on clays)

$T = 298.15\ K \cdots 348.15\ K\ (25^oC \cdots 75^oC)$

$\rho = 1000\ kg / m^3$

$\nabla h = 1$

Notice that the largest uncertainty is given by the large range of values for the thermo-osmotic permeability. With these considerations taken into account, the range of values for the thermal filtration heat flux is

$$|J_{TF}| : 3\times10^{-8} \cdots 3\times10^{-4}\ J / m^2 / s$$

The simplest way to evaluate these estimates is to compare them with the thermal conduction heat flux, which is described by

$$J_{TC} = -\kappa \nabla T \qquad (4.6)$$

where κ is the thermal conductivity of the medium. Thermal conductivities for the Opalinus Clay range from 1 to 2.6 W/m/K (NAGRA, 1984, 1989b; NAGRA, unpublished measurements).

The heat fluxes caused by thermal filtration (Eqn. 4.5) and thermal conduction (Eqn. 4.6) will be equal in absolute value when

$$\left|\frac{\nabla T}{\nabla h}\right| = \frac{k_T T \rho g}{\kappa} \approx 10^{-8} \cdots 3\times10^{-4}\ K / m$$

Expressed in other terms, the thermal conduction heat flux will be larger in magnitude than the thermal filtration flux when $|\nabla T| > (10^{-8} \cdots 3\times10^{-4}) \times |\nabla h|$. Therefore, thermal conduction will be far more important than thermal filtration given any relevant temperature gradient**.** Notice, for instance, that the average global geothermal gradient is about 0.03 K/m, and that a temperature gradient one order of magnitude smaller than that would still cause thermal filtration to be clearly negligible, for hydraulic gradients about unit $(\nabla h \approx 1)$.

4.2 The Dufour effect

The term Dufour effect applies to the heat flux caused by chemical potential gradients. The lack of experimental observations will also lead in this case to the use of the Onsager Reciprocal Relations (ORR) to obtain values for the phenomenological coefficients associated with the Dufour effect (L_{qk}).

The thermal diffusive flux of species i, which is related by ORR to the Dufour effect, is given by

$$J_{TD} = -D_e s c_i \nabla T \tag{4.7}$$

where D_e is the effective diffusion coefficient, s is the Soret coefficient, and c_i is the mass concentration of species i. The same flux can be written, according to irreversible thermodynamics, as

$$J_{TD} = -L_{iq} \frac{\nabla T}{T^2} \tag{4.8}$$

Combining Eqns. 4.7, 4.8, and 2.4, the phenomenological coefficients for the Dufour effect can be calculated according to

$$L_{qi} = D_e s c_i T^2 \tag{4.9}$$

The heat flux associated with the Dufour effect, in units of energy per total cross-section area per time, is given by

$$J_{DE} = -\sum_{i=1}^{n} \frac{L_{qi}}{W_i} \nabla\left(\frac{\mu_i}{T}\right) = -\sum_{i=1}^{n} \frac{D_e s c_i}{W_i} T^2 \nabla\left(\frac{\mu_i}{T}\right) \tag{4.10}$$

and again, assuming that the temperature gradient is sufficiently small, Eqn. 4.10 can be rewritten as

$$J_{DE} = -\sum_{i=1}^{n} \frac{D_e s c_i}{W_i} T \nabla \mu_i \tag{4.11}$$

This flux is a summation over the contributions arising from each individual species i in solution (each species contributes to the flux with its own phenomenological coefficient L_{qi} and chemical potential gradient $\nabla\mu_i$). At this point it is convenient to introduce some simplifications. First, temperature will again be assumed to be constant, which is quite reasonable given the low temperature gradients (about 0.25 K/m) expected in the vicinity of the repository at the time of waste canister failure ($t \approx 1000$ y, SATO et al., 1998). Then, the solution will be assumed to be ideal (unit activity coefficients), so chemical potential gradients are given by

$$\nabla \mu_i = \frac{RT}{c_i} \nabla c_i \tag{4.12}$$

and Eqn. 4.11 can be rewritten as

$$J_{DE} = -\sum_{i=1}^{n} \frac{D_e s R T^2}{W_i} \nabla c_i \tag{4.13}$$

The validity of these assumptions will be further discussed after the estimates for the heat flux associated with the Dufour effect have been calculated. Now, the phenomenological coefficients for the different species in solution will be assumed to be all the same (a conservative large value will be used for all the species). The result is that only one “average” species in solution will be considered in the calculations, and the heat flux caused by the Dufour effect will be written as

$$J_{DE} = -\frac{D_e s R T^2}{\overline{W}} \nabla c_{tot} \tag{4.14}$$

where $\overline{W}$ is the concentration-weighted average molar weight calculated over all the species in solution, and c_{tot} is the total concentration in solution

$$c_{tot} = \sum_{i=1}^{n} c_i \tag{4.15}$$

The parameters that will be used to calculate an estimate of the heat flux caused by the Dufour effect are again intended to simulate the conditions in the vicinity of the repository for vitrified high level waste and spent fuel hosted by the Opalinus Clay. These parameters are:

$$D_e = 10^{-11}\ \mathrm{m^2/s}$$
$$s = 10^{-2}\ \mathrm{K^{-1}}$$
$$T = 298.15\ \mathrm{K} \cdots 348.15\ \mathrm{K}$$
$$\overline{W} = 0.03\ \mathrm{kg/mol}$$

Conservatively large values have been chosen for the effective diffusion coefficient (D_e) and the Soret coefficient (s). The value of the average molar weight $(\overline{W})$ is approximately the value for a NaCl solution (Na and Cl are, together with sulfate, the main components of groundwater in Opalinus Clay; see GAUTSCHI et al., 1993). However, since there are other species in solution, the average molar weight should be higher. The fact that this molar weight is in the denominator of Eqn. 4.14 means that the use of a relatively small value for $\overline{W}$ results in a conservative estimate (the calculated heat flux will tend to be too high).

Regarding the concentration gradient, the same approach used in section 3.3.2 will be applied here. Assuming a total solute concentration (c_{tot}) in the Opalinus Clay of 20 kg/m^3 (GAUTSCHI et al., 1993), a possible range of concentration gradients can be expressed by a change in c_{tot} from 0 to 20 kg/m^3 over a distance of 1, 10, or 100 m. The resulting concentration gradient (∇c_{tot}) will be 20, 2, or 0.2 kg/m^3/m, respectively.

The heat fluxes caused by the Dufour effect (Eqn. 4.14) and thermal conduction (Eqn. 4.6) will be equal in absolute value when

$$\left|\frac{\nabla T}{\nabla c_{tot}}\right| = \frac{D_e s R T^2}{\kappa \overline{W}} \approx 10^{-6} \cdots 3\times10^{-6}\ \mathrm{K\cdot m^3 / kg}$$

given the range of values for the thermal conductivity of the Opalinus Clay, which goes from 1 to 2.6 W/m/K. Therefore, thermal conduction will be more important than the Dufour effect when $|\nabla T| > (10^{-6} \cdots 3\times10^{-6})\times\left|\nabla c_{tot}\right|$. Using the concentration gradients discussed above (∇c_{tot} between 0.2 and 20 kg/m^3/m), it can readily be seen that for any relevant temperature gradient, the heat flux caused by the Dufour effect will be negligible compared to thermal conduction. Actually, the difference in magnitude between the two fluxes is so large (several orders of magnitude), that the assumption of ideality for the solution (unit activity coefficients) becomes absolutely non-critical, given the range of solution compositions found in the Opalinus Clay.

5. SIMPLE ONE-DIMENSIONAL TRANSPORT SIMULATIONS INCLUDING THERMAL AND CHEMICAL OSMOSIS, HYPERFILTRATION, AND THERMAL DIFFUSION.

After having shown that the contribution of thermal filtration and the Dufour effect to heat transport in the Opalinus Clay is negligible, the solute fluxes associated with the other transport phenomena will be combined into a simple one-dimensional transport model to obtain additional information on the combined effect of the different coupled transport phenomena and their potential contributions to solute transport.

5.1 The transport equation

The solute fluxes (kg/m^2/s) associated with advection, chemical diffusion, chemical osmosis, hyperfiltration, thermal diffusion, and thermal osmosis are given by Eqns. 3.1 to 3.6. If the hydraulic head (∇h), osmotic pressure head ($\nabla \Pi_h$), and temperature gradients (∇T) are assumed to be constant along a one-dimensional section of the Opalinus Clay, and assuming also constant porosity (ϕ), effective diffusion coefficient (D_e), hydraulic conductivity (K), osmotic efficiency (σ), Soret coefficient (s), and thermo-osmotic permeability (k_T), all the fluxes can be incorporated into a transport equation of the form

$$\frac{\partial c_i}{\partial t} = \mathrm{D}\frac{\partial^2 c_i}{\partial x^2} - \mathrm{v}\frac{\partial \mathrm{c_i}}{\partial \mathrm{x}} \tag{5.1}$$

where

$$\mathrm{D} = \frac{D_e}{\phi} \tag{5.2}$$

and

$$\mathrm{v} = \frac{-K\frac{\partial h}{\partial x} + \sigma K\frac{\partial \Pi_h}{\partial x} + \sigma K\frac{\partial h}{\partial x} - D_e s\frac{\partial T}{\partial x} - k_T\frac{\partial T}{\partial x}}{\phi} \tag{5.3}$$

The assumption of constant gradients is intended only to allow the estimation of the relative role of the different transport phenomena under different conditions (sets of parameter values).

The release of a tracer from a repository hosted by the Opalinus Clay can be simulated by making use of Eqn. 5.1 with the following initial and boundary conditions:

$$c(x,0) = 0 \qquad x \geq 0$$
$$c(0,t) = c_0 \qquad t \geq 0$$
$$c(\infty,t) = 0 \qquad t \geq 0$$

The analytical solution to Eqn. 5.1 with the initial and boundary conditions described above was reported by OGATA & BANKS (1961) and is given by

$$\frac{c}{c_0} = \frac{1}{2}\left[\operatorname{erfc}\left(\frac{x - \mathrm{v}t}{2\sqrt{\mathrm{D}t}}\right) + \exp\left(\frac{\mathrm{v}x}{\mathrm{D}}\right)\operatorname{erfc}\left(\frac{x + \mathrm{v}t}{2\sqrt{\mathrm{D}t}}\right)\right] \tag{5.4}$$

5.2 Simulations

A series of simulations have been run with the objective of estimating the effects of the different coupled transport phenomena within the reference frame of a one-dimensional transport calculation. The parameters of the model intend to simulate the conditions in the vicinity of a repository for vitrified high level waste (HLW) and spent nuclear fuel (SF) hosted by the Opalinus Clay at the estimated time of waste canister failure (t ≈ 1000 y).

5.2.1 Model parameters

5.2.1.1 Hydraulic, temperature, and osmotic pressure head gradients

A unit hydraulic gradient $\left(\partial h/\partial x = -1\right)$ has been assumed, based on measured hydraulic heads in Opalinus Clay and in aquifers above and below Opalinus Clay (NAGRA, 1994). Also, based on model calculations by SATO et al. (1997) regarding thermal gradients in the vicinity of the repository, a temperature gradient of 0.25 K/m ($\partial T/\partial x = -0.25$ K/m) has been used. Both hydraulic and temperature gradients are negative so they promote transport by advection, thermal diffusion, and thermal osmosis in the direction of increasing x.

Concerning the osmotic pressure head gradient, calculations have been performed with values of $\partial \Pi_h/\partial x = 1$ and $\partial \Pi_h/\partial x = 10$, which correspond to salinity gradients equivalent to the change between OPA groundwater and a dilute solution occurring in a distance of 100 m and 10 m, respectively (see section 3.5.1). Positive gradients imply that the chemical osmotic flux will be in the direction of increasing x (the same direction as advection, thermal diffusion, and thermal osmosis).

5.2.1.2 Other parameters

Hydraulic conductivity (K) values of 10^{-13} and 10^{-12}m/s, and effective diffusion coefficients (D_e) of 10^{-12} and 10^{-11} m^2/s have been used, given the range of reasonable values assumed for OPA (section 3.2). A porosity (ϕ) of 0.05 has been used in the calculations. The value of the osmotic efficiency coefficient

(σ) has been set to 0.1, based on measurements on OPA samples by HARRINGTON & HORSEMAN (1999). However, results for other values of σ will also be shown. The values of the Soret coefficients and thermo-osmotic permeabilities are based on the range of possible values for OPA (sections 3.6 and 3.7). All the results that will be shown correspond to t = 5000 y after initial release (waste canister failure). This point in time was arbitrarily chosen, but is in the range of times before temperatures go significantly down in the repository (SATO et al., 1998).

5.2.2 Results and discussion

Figure 5.1 shows concentration (as c/c_0) vs. distance at t = 5000 y, for four different values of the thermo-osmotic permeability (k_T). The other parameters characterizing this set of calculations are $K = 10^{-13}$ m/s, $D_e = 10^{-12}$ m^2/s, $s = 0$, $\partial\Pi_h/\partial x = 1$, and $\sigma = 0.1$. Notice that the fact that the hydraulic and osmotic pressure head gradients are -1 and 1, respectively, means that the hyperfiltration and chemical osmotic fluxes cancel each other (see Eqns. (3.4 and 3.3), and also that the results are independent of the value of σ.

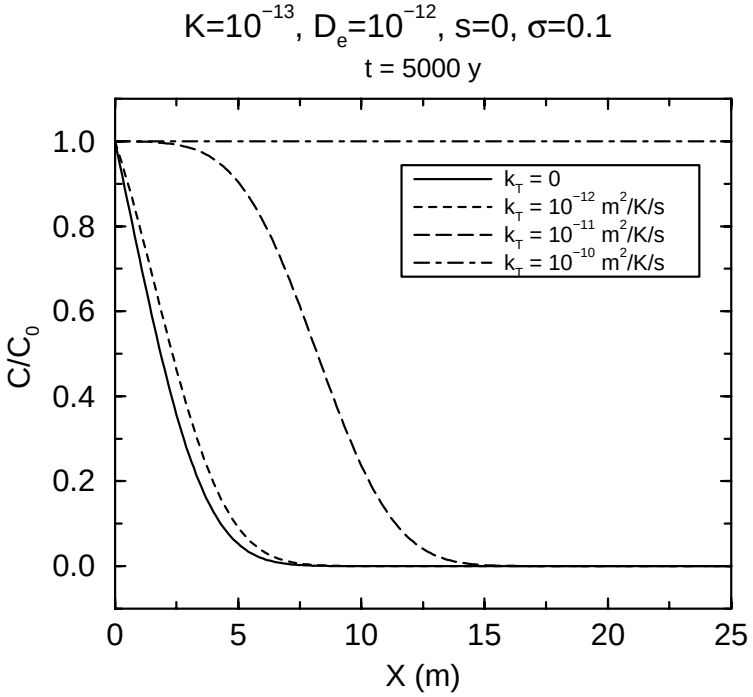

Figure 5.1: Relative concentration vs. distance at t = 5000 y. The different curves correspond to different values of the thermo-osmotic permeability k_T. Thermal osmosis will only have a significant effect if $k_T > 10^{-12}$ m^2/K/s.

The results show thermal osmosis will have a significant effect if $k_T > 10^{-12}$ m^2/K/s. Notice that the range of possible values of k_T, based on experimental studies on compacted clays, goes between 10^{-14} and 10^{-10} m^2/K/s (see section 3.7). Therefore, there is a potential for thermal osmosis having a strong impact on solute and fluid transport under these conditions.

Figures 5.2(a) and 5.2(b) show the same type of calculation, but for different values of K and D_e. The results in Fig. 5.2(a), which correspond to the case where $K = 10^{-12}$ m/s, show that the effect of the increased hydraulic conductivity is quite minor (the system is not advection-dominated), and also that thermal-osmosis will have a significant effect for $k_T > 10^{-12}$ m^2/K/s. The same conclusion can be drawn from the results shown in Fig. 5.2(b), which corresponds to the case with $D_e = 10^{-11}$ m^2/s.

The results of an evaluation of the potential effect of thermal diffusion on solute transport are shown in Fig. 5.3. The solid line corresponds to the case where the only transport mechanisms are advection and chemical diffusion. The dashed line shows the additional effect of thermal diffusion, characterized by a Soret coefficient (s) of 0.1 K^{-1}. Notice that even with this large value of s, which is about one order of magnitude larger that any reported value, the effect is negligible.

The effect of chemical osmosis can be observed from the results shown in Figs. 5.4(a) and 5.4(b). An osmotic pressure head gradient ($\partial\Pi_h/\partial x$) of 10 has been used, so the chemical osmosis and hyperfiltration fluxes do not cancel each other (see Eqns. 3.3 and 3.4). A value of 10 for the osmotic pressure head gradient is roughly equivalent to the change between OPA groundwater and a dilute solution occurring in a distance of 10 m. Notice that this salinity gradient is quite steep, and that a salinity gradient that were any steeper could only be maintained for very small distances through the rock (<<10 m).

Comparing Figs. 5.1 and 5.4(a) it can be seen that the additional effect of chemical osmosis on solute transport is quite negligible. Furthermore, the possibility that the Opalinus Clay were characterized by larger osmotic efficiencies ($\sigma > 0.1$) is considered in Fig. 5.4(b). The different curves correspond to different values of σ. Thermal diffusion and thermal osmosis are not considered in this case. It can be observed that even in the improbable case of ideal efficiency ($\sigma = 1$) and high prevailing osmotic pressure head gradient ($\partial\Pi_h/\partial x = 10$), the effect of chemical osmosis is rather minor, especially compared to the potential effect of thermal osmosis (see Fig. 5.4(a)).

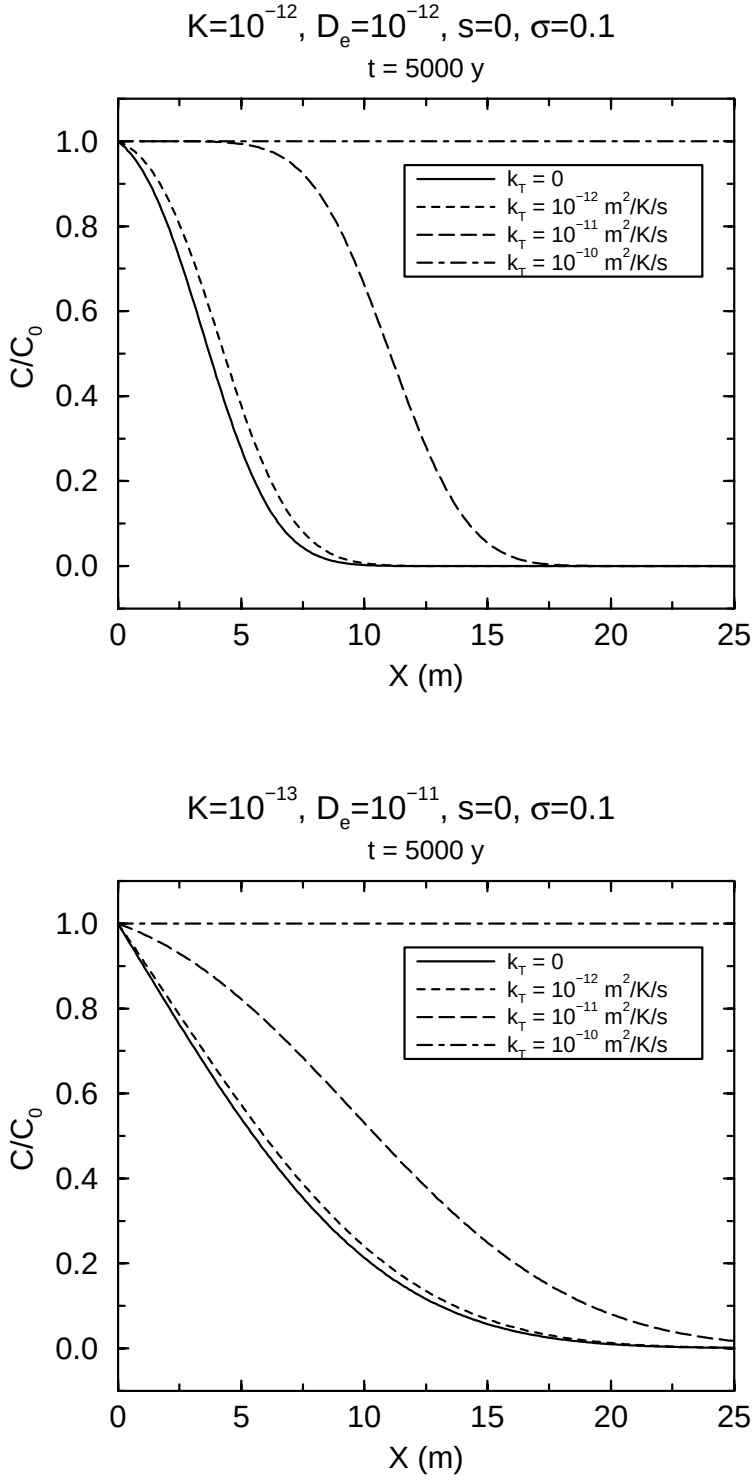

Figure 5.2: Relative concentration vs. distance at t = 5000 y, for (a) hydraulic conductivity K equal to 10^{-12} m/s, and (b) effective diffusion coefficient D_e equal to 10^{-11} m^2/s. The different curves in both plots correspond to different values of the thermo-osmotic permeability k_T.

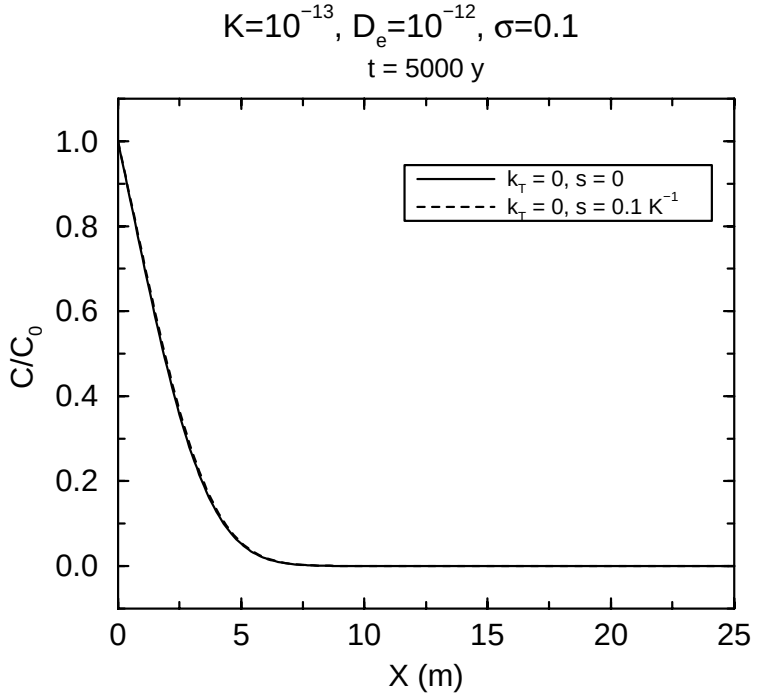

Figure 5.3: Relative concentration vs. distance at t = 5000 y, for two different values of the Soret coefficient (s = 0 and s = 0.1 K^{-1}).

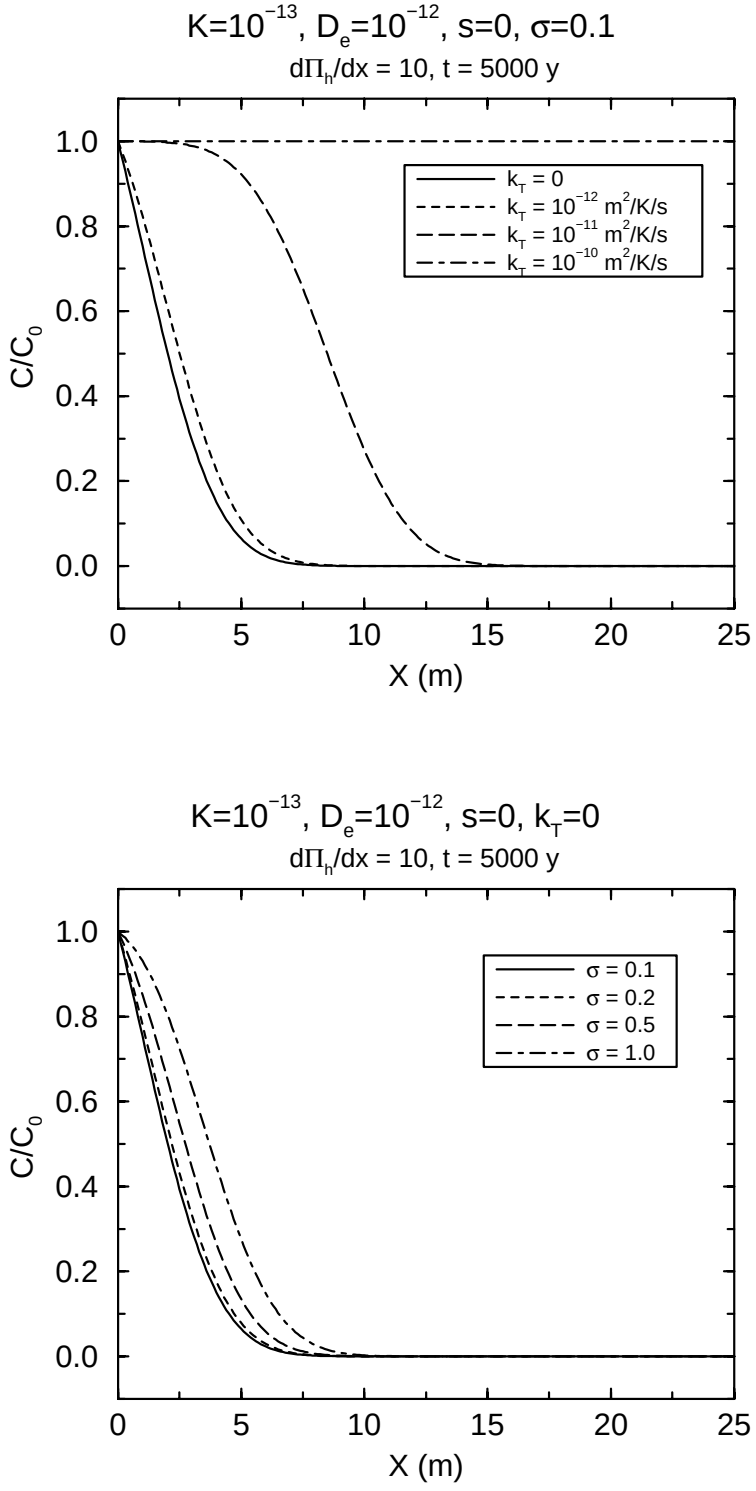

Figure 5.4: Relative concentration vs. distance at t = 5000 y, for the case with an osmotic pressure head gradient $\left(\partial \Pi_h / \partial x\right)$ equal to 10. (a) Results for different values of the thermo-osmotic permeability k_T. (b) Results for different values of the osmotic efficiency σ, with $k_T = 0$.

6. COUPLING BETWEEN ADVECTION AND THERMAL OSMOSIS: TWO- AND THREE-DIMENSIONAL FLOW CALCULATIONS.

In the previous sections it has been shown that thermal osmosis is the only coupled transport mechanism that could have a strong impact on fluid and solute transport in the vicinity of a repository hosted by the Opalinus Clay. The contribution of thermal osmosis to fluid and solute transport can be significant if its effect is simply added to the other transport mechanisms. However, since thermal osmosis is a flux of fluid, conservation of fluid mass has to be taken into account in order to make any accurate predictions about its role in the performance of a nuclear waste repository. Thermal osmosis promotes the transport of fluid down the temperature gradient, and would therefore cause groundwater to move away from the repository (the heat source) in all directions. It is clear that without an extra source of solution, transport will be limited by the available amount of fluid in the system (conservation of fluid mass).

Two- and three-dimensional flow models including advection and thermal osmosis have been developed. The results from model simulations allow the evaluation of the effect of thermal osmosis when conservation of fluid mass and conservation of energy are taken into account. Additional two-dimensional simulations including temperature-dependent fluid density and viscosity terms have also been run.

6.1 Two-dimensional model

6.1.1 Model formulation

The model that will be used solves numerically the equations of conservation of fluid mass and conservation of energy at steady state, for constant porosity and fluid density, in an homogeneous and isotropic porous medium. Observations from ten motorway and railway tunnels in which the Opalinus Clay is exposed have shown no water flow through the formation, including fractured zones, for sections with more than 200 m of overburden (GAUTSCHI, 1997). Also, field tests at the Mont Terri Underground Rock Laboratory have shown that there is no significant contrast in terms of hydraulic properties between a major fault zone and the wall rock (WYSS, MARSCHALL & ADAMS, 1999). These observations are consistent with the assumption of an homogeneous and isotropic medium for the flow model.

The model intends to simulate the conditions near the repository at the time of waste canister failure. Previous model calculations (SATO et al., 1998) suggest that temperature gradients in the vicinity of the repository will be rather low at the time of canister failure (gradients less than 1 K/m, and probably of the order

of 0.25 K/m, at t ≈ 1000 y). These results led to the assumption of steady state and constant fluid density.

The equations of conservation of fluid mass and conservation of energy are written as

$$\nabla \cdot v = 0 \tag{6.1}$$

and

$$\nabla \cdot \kappa \nabla T - \rho c_f \nabla \cdot (vT) + A = 0 \tag{6.2}$$

respectively, where v, the total specific discharge or total flow velocity, which has units of m^3/m^2rock/s, is given by

$$v = -K \nabla h - k_T \nabla T \tag{6.3}$$

The first term on the right-hand-side of Eqn. 6.3 corresponds to Darcy's law (advection), and the second term describes the contribution to the total specific discharge from thermal osmosis. κ, K, and k_T are the thermal conductivity, hydraulic conductivity, and thermo-osmotic permeability of the porous medium, respectively. They are all assumed to be constant. ρ and c_f are the density and heat capacity at constant pressure of the fluid, and are also assumed to be constant. A is the heat source term, and h and T are the hydraulic head and temperature, respectively.

The system composed of Eqns. 6.1 and 6.2 is numerically solved for the hydraulic heads (h) and temperature (T), and fluid velocities are then calculated according to Eqn. 6.3. The spatial discretization of the system is done according to a cell-centered finite difference scheme. The resulting system of algebraic nonlinear equations is solved using Newton's method.

The flow domain (Figure 6.1) is a square, where constant hydraulic heads and temperatures are specified at the nodes on the exterior side of all the boundaries. Hydraulic head and temperature on the left- and right-hand-side boundaries are constant along the boundary, defining overall gradients from one side to the other of the domain. Hydraulic heads and temperatures along the top and bottom boundaries change linearly with space between their values on the left- and right-hand-side boundaries.

6.1.2 Results and discussion

Two different sets of results are shown in Figs. 6.2 and 6.3, corresponding to two different overall temperature differences between left- and right-hand-side boundaries. In the first case (Fig. 6.2) the temperature is the same in both sides, and in the second one (Fig. 6.3) the temperature on the left-hand-side is about one degree higher than on the right-hand-side. In both cases there is a

unique (only one node) heat source at the center of the domain. The value of the heat source was arbitrarily chosen to produce relatively low temperature gradients.

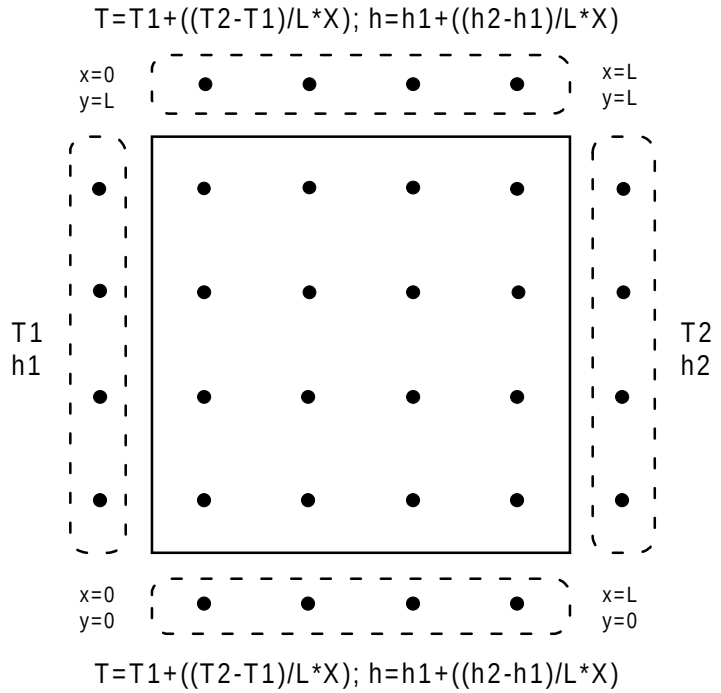

Figure 6.1: Schematic diagram showing the geometry and boundary conditions of the flow domain used in the model. The flow domain is enclosed by a thick solid line. External nodes, where the boundary conditions are defined, are enclosed by dashed lines.

The parameters for both simulations are:

L = 16 m; 1 m spacing between nodes

h1 = 25 m; h2 = 9 m (overall unit hydraulic gradient from left to right)

T1 = T2 = 298.15 K (case shown in Fig. 6.2)

T1 = 299.22 K; T2 = 298.08 K (case shown in Fig. 6.3)

K = 10^{-9} m/s

k_T = 10^{-6} m^2/K/s

κ = 2.6 W/m/K

A = 20 $J/m^3/s$ (only in one node at the center of the domain)

ρ = 1000 kg/m^3

c_f = 4180 J/kg/K

The values of the hydraulic conductivity (K) and thermo-osmostic permeability (k_T) are certainly too high compared to the values that would apply to the Opalinus Clay (see sections 3.2 and 3.7). These values were used because they provided good convergence of the numerical calculations. It should be emphasized that the goal of the calculations in this section is to study how the coupling between advection and thermal osmosis works, rather than obtaining specific values for the flow velocities.

6.1.2.1 Case 1 (T1 = T2 = 298.15 K)

Figure 6.2(a) shows the calculated temperature distribution in the system. Figures 6.2(b), 6.2(c), and 6.2(d) show the total flow velocity, the advective component of the total flow velocity ($-K\nabla h$), and the thermal-osmotic component ($-k_T\nabla T$), respectively. Notice that thermal osmosis promotes fluid transport down the temperature gradient (from the center of the domain outwards). However, and due to the fact that there is no extra source of fluid in that region of the flow domain, the resulting hydraulic gradient causes the advective component ($-K\nabla h$) to oppose thermal osmosis. The result is that there is no net effect of thermal osmosis. The total flow velocity field is homogeneous (no component of velocity in the y direction), and the magnitude of the total velocity at all points equals the hydraulic conductivity (K) times the overall hydraulic gradient ((h2-h1)/L).

6.1.2.2 Case 2 (T1 = 299.22 K, T2 = 298.08 K)

Figure 6.3(a) shows the calculated temperature distribution in the system. Figures 6.3(b), 6.3(c), and 6.3(d) show the total flow velocity, the advective component of the total flow velocity ($-K\nabla h$), and the thermal-osmotic component ($-k_T\nabla T$), respectively. Notice again that thermal osmosis promotes fluid transport down the temperature gradient (from the center of the domain outwards), and also, that there is an extra component of thermal osmosis in the x direction, caused by the temperature difference between the left- and right-hand-side boundaries (the streamlines curve to the direction of increasing x near the top and bottom boundaries). As in the previous case, and due to the fact that there is no extra source of fluid in the interior of the flow domain, the resulting hydraulic gradient causes the advective component ($-K\nabla h$) to cancel the disturbance in the flow field caused by thermal osmosis, and the end result is that there is no net effect of thermal osmosis arising from the presence of a heat source in the interior of the domain. The total flow velocity field is homogeneous (no component of velocity in the y direction). The only effect of thermal osmosis is to change the magnitude of the total velocity. The total velocity at all points is now given by

$$v = -K\,((h2-h1)/L) - k_T\,((T2-T1)/L)$$

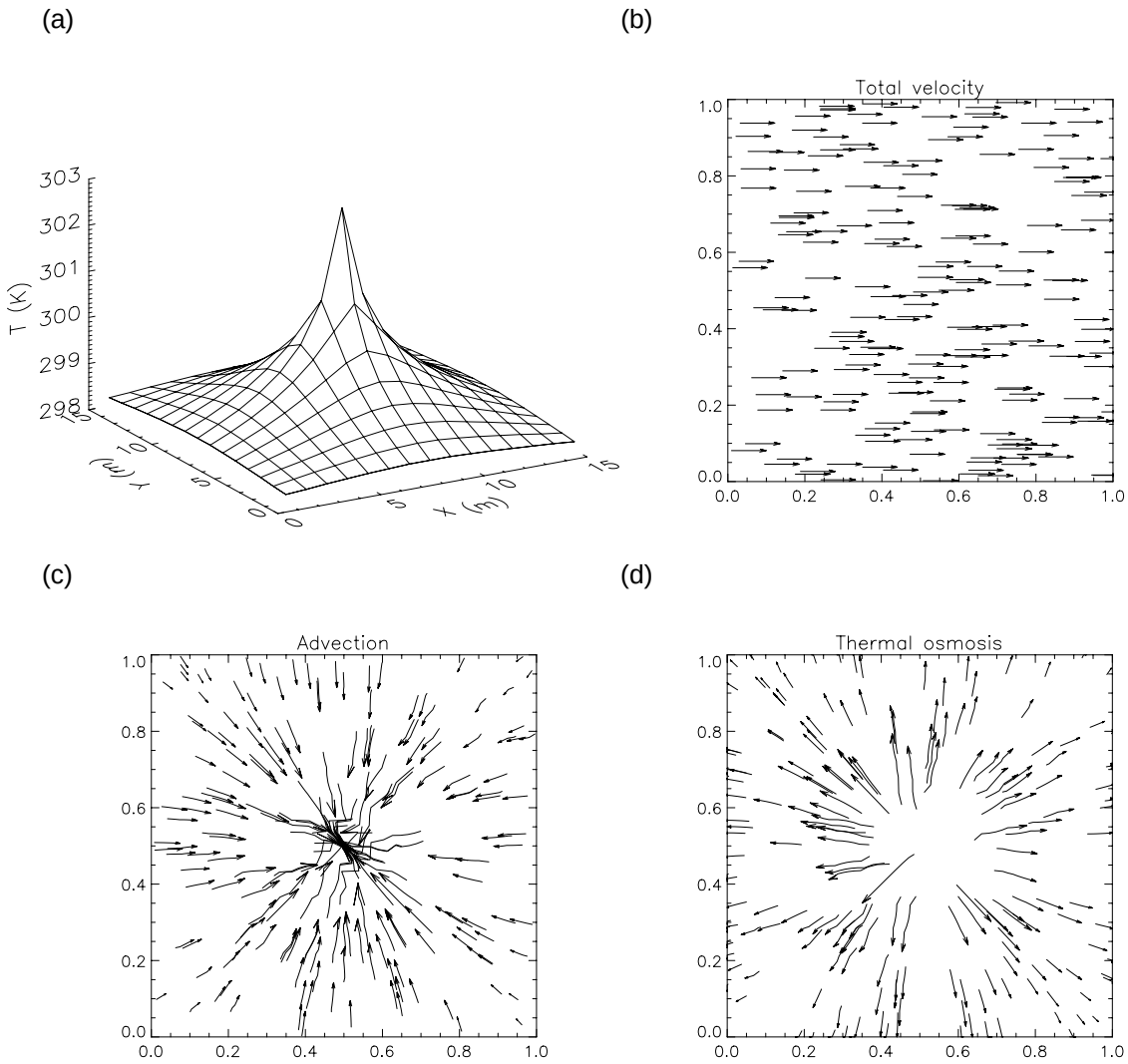

Figure 6.2: Results for case 1 (T1 = T2 = 298.15 K). (a) Temperature, (b) total specific discharge, (c) advective component of the total specific discharge, and (d) thermal-osmotic component of the total specific discharge. Notice how the advective component of flow cancels the thermal-osmotic component, and there is no net effect of thermal osmosis on the flow field.

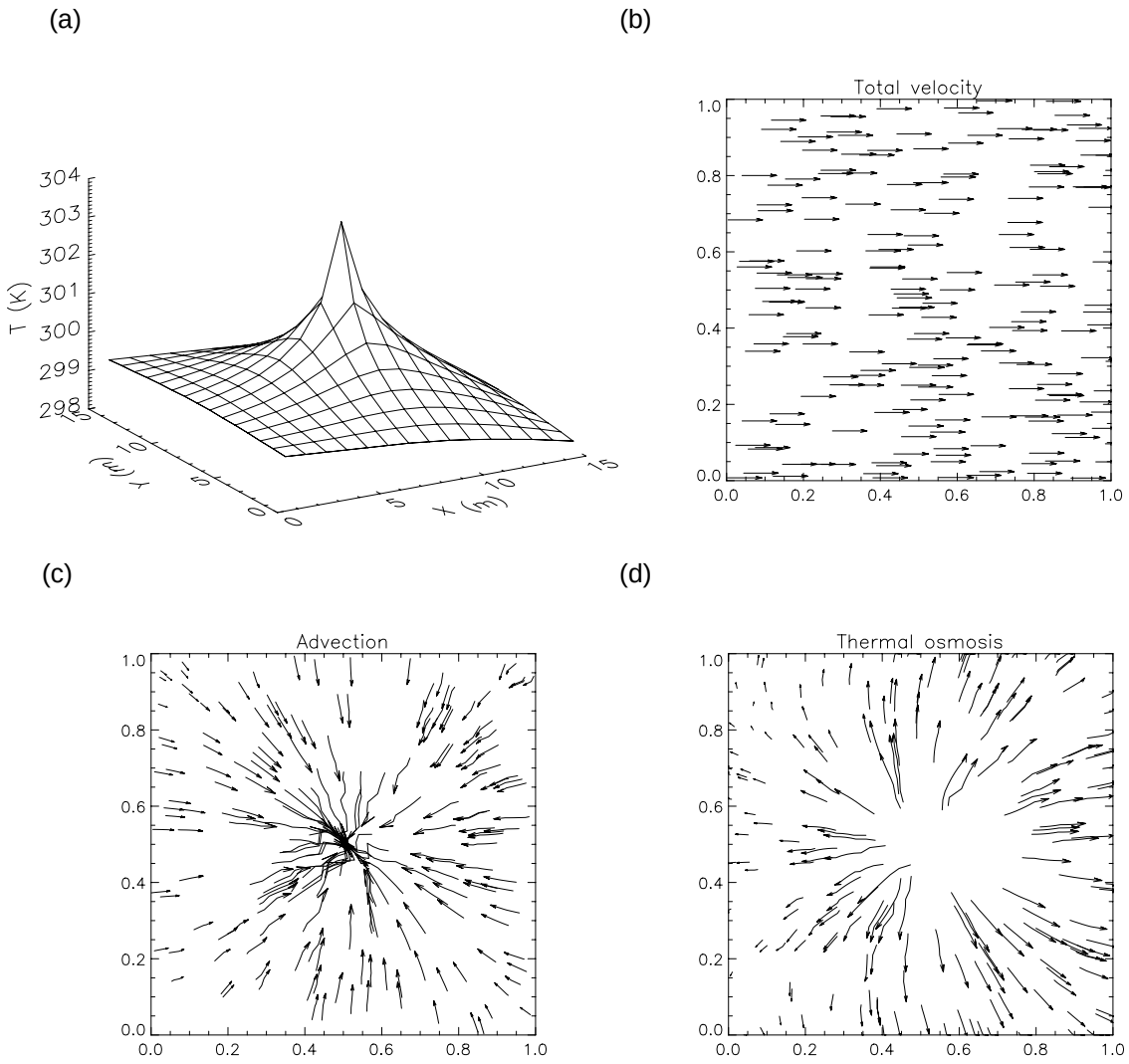

Figure 6.3: Results for case 2 (T1 = 299.22 K, T2 = 298.08 K). (a) Temperature, (b) total specific discharge, (c) advective component of the total specific discharge, and (d) thermal-osmotic component of the total specific discharge. Notice how the advective component of flow cancels the thermal-osmotic component, and there is no net effect of thermal osmosis arising from the presence of a heat source in the interior of the domain on the flow field.

6.2 Three-dimensional model

The possible effect of thermal osmosis when three-dimensional flow is taken into account has been evaluated by running a three-dimensional version of the model described in the previous section.

6.2.1 Model formulation

This model is identical in its formulation to the two-dimensional model described in section 6.1.1. The same equations and the same numerical approach are used. The only difference is the addition of the third dimension in the calculations.

The flow domain is a parallelopiped (Fig. 6.4), where constant hydraulic heads and temperatures are specified at the nodes on the exterior side of all the boundaries (the same approach shown in Fig. 6.1).

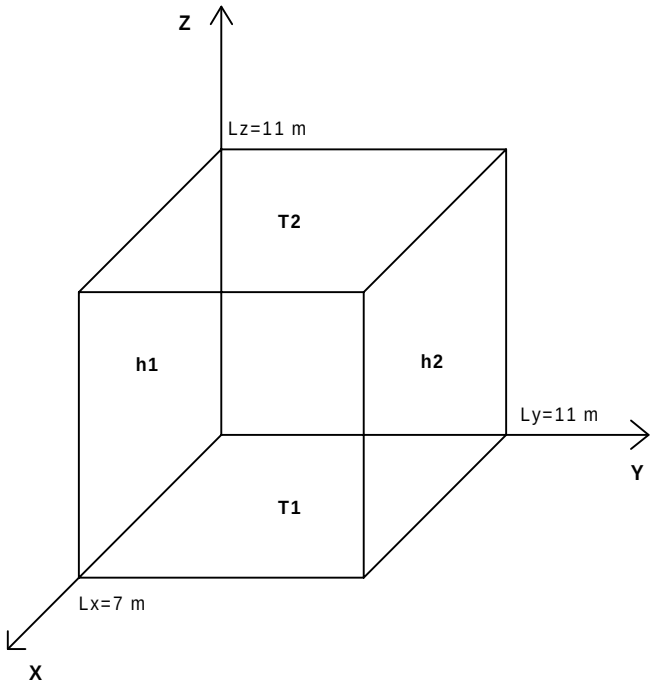

Figure 6.4: Schematic representation of the three-dimensional flow domain used in the model.

The results of two different simulations will be shown. In the first case, hydraulic heads on the left- and right-hand-side boundaries are constant along the boundary, defining an overall gradient along the y direction from one side to the other of the domain. In the second case, an overall temperature gradient along the z direction is added to the problem.

6.2.2 Results and discussion

The parameters for both simulations are:

Dimensions: L_x = 7 m; L_y = L_z = 11 m.

Finite difference grid spacing: 1m spacing between nodes in all directions.

h1 = 20.5 m; h2 = 9.5 m (overall unit hydraulic gradient from left to right)

T1 = T2 = 298.15 K (case 1)

T1 = 299.20 K; T2 = 298.10 K (case 2)

K = 10^{-9} m/s (case 1)

K = 10^{-7} m/s (case 2)

k_T = 10^{-6} m/s

κ = 2.6 W/m/K

A = 20 J/m^3/s (only in one node at the center of the domain)

ρ = 1000 kg/m^3

c_f = 4180 J/kg/K

As it was the case in the two-dimensional simulations, the values of the hydraulic conductivity (K) and thermo-osmotic permeability (k_T) are too high to be representative of the transport properties of the Opalinus Clay. These values were used because they provided good convergence of the numerical calculations. Again, it has to be emphasized that the goal of the calculations is to show how the coupling between advection and thermal osmosis works, rather than obtaining specific values for the two components of the flow velocity.

6.2.2.1 Case 1 (T1 = T2 = 298.15 K)

The results are shown in Figs. 6.5, 6.6 and 6.7. Figure 6.5 shows temperature and flow velocities in a section of the flow domain perpendicular to the x axis and going through the center of the domain. Figures 6.6 and 6.7 correspond to sections perpendicular to the y and z axes, respectively, and going also through the center of the domain. In all the figures it is easily observed that the advective component of flow compensates for the disturbance caused in the flow field by the thermal-osmotic component. The end result is that there is no net effect of thermal osmosis. The flow field is homogeneous, with water flowing down the overall hydraulic gradient (parallel to the y axis). The apparent

randomness of the total flow velocity field in the section perpendicular to the y axis (Fig. 6.6b) is just due to a numerical effect. The magnitudes of the components of the total flow velocity in the x and z directions are of the order of 10^{-20} m/s (they are effectively zero). The total flow velocity at all points is given by

$$v = -K\left(\frac{\mathrm{h2 - h1}}{\mathrm{L_y}}\right)$$

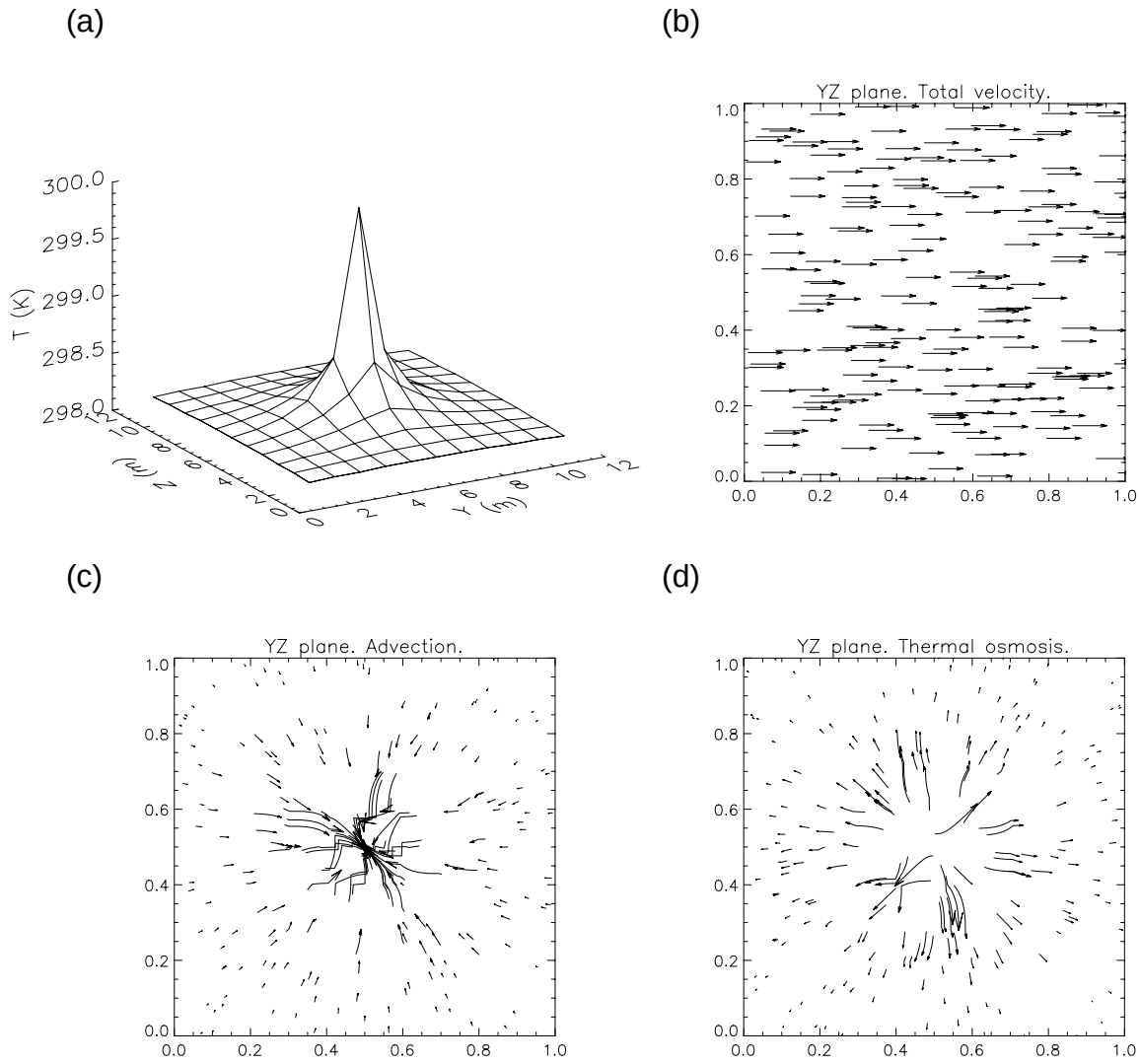

Figure 6.5: Results for case 1 (T1 = T2 = 298.15 K) in a section of the flow domain perpendicular to the x axis and going through the center of the domain. (a) Temperature, (b) total flow velocity, (c) advective component of the total velocity, and (d) thermal-osmotic component of the total velocity. Notice how the advective component of flow cancels the thermal-osmotic component, and there is no net effect of thermal osmosis on the flow field. The flow field is homogeneous, with fluid flowing in the y direction, down the overall hydraulic gradient.

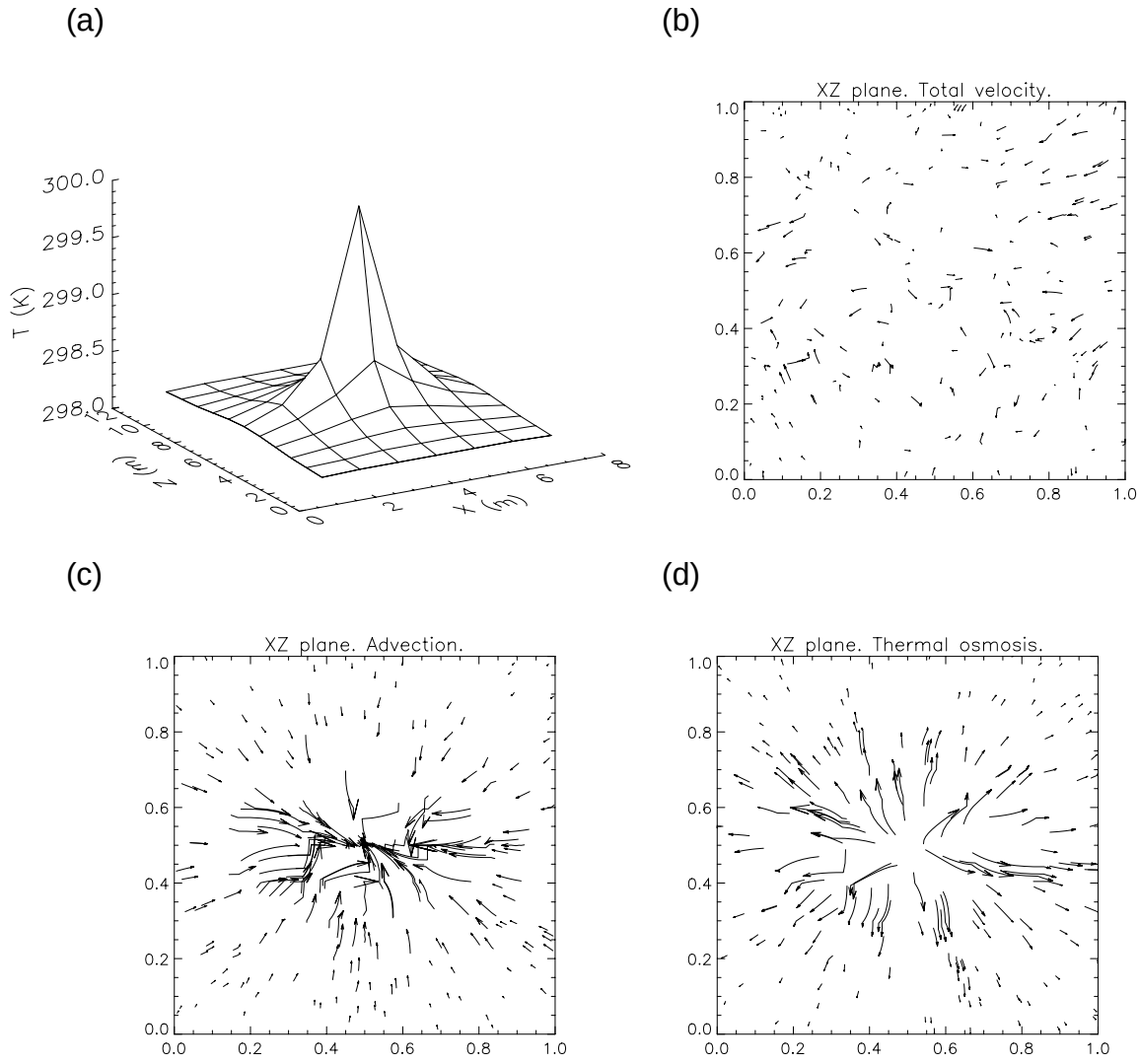

Figure 6.6: Results for case 1 (T1 = T2 = 298.15 K) in a section of the flow domain perpendicular to the y axis and going through the center of the domain. (a) Temperature, (b) total flow velocity, (c) advective component of the total velocity, and (d) thermal-osmotic component of the total velocity. Notice how the advective component of flow cancels the thermal-osmotic component, and there is no net effect of thermal osmosis on the flow field. The apparent randomness of the total flow velocity field in this section is due to a numerical effect. The magnitudes of the components of the total flow velocity in the x and z directions are of the order of 10^{-20} m/s (they are effectively zero).

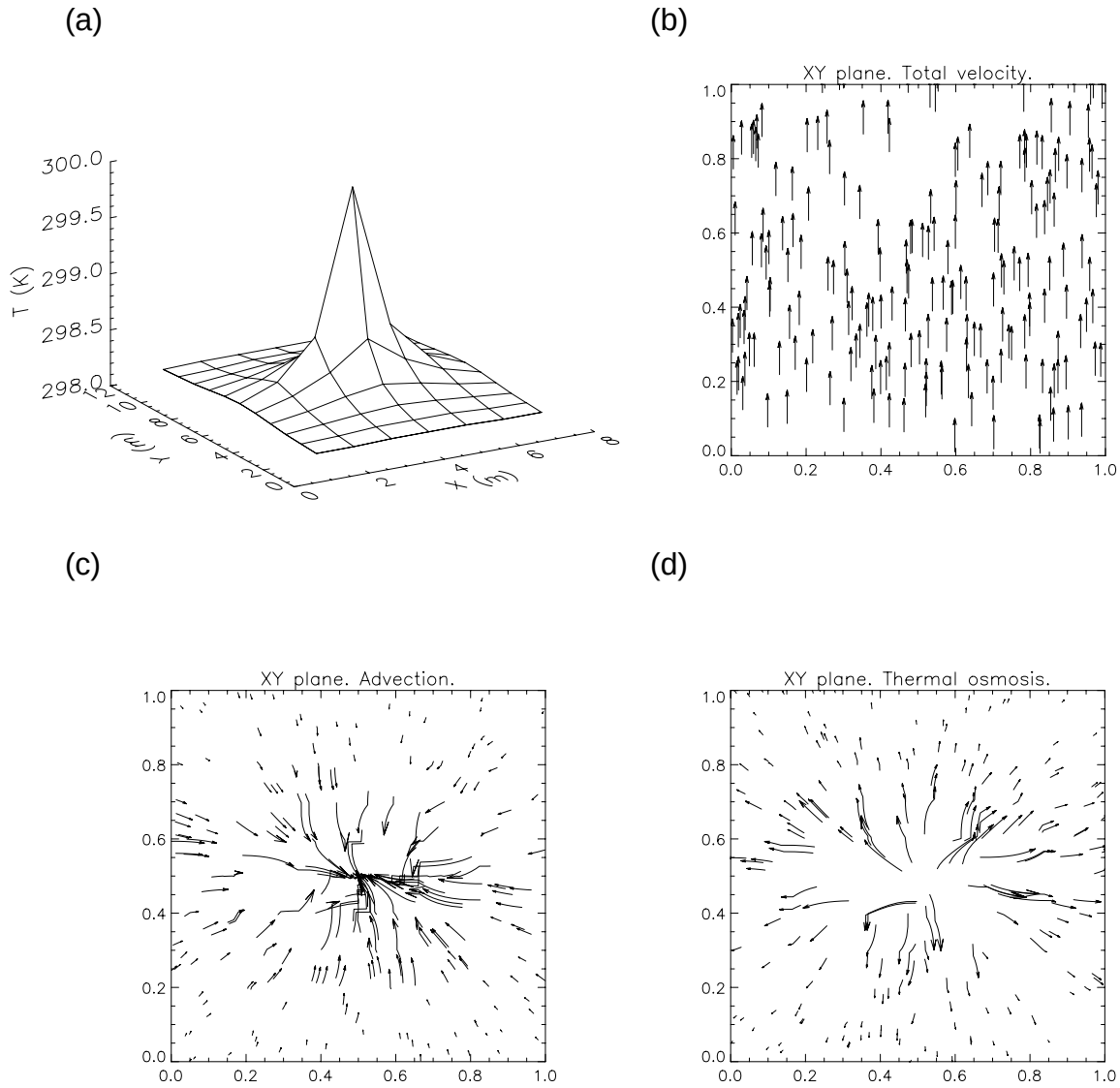

Figure 6.7: Results for case 1 (T1 = T2 = 298.15 K) in a section of the flow domain perpendicular to the z axis and going through the center of the domain. (a) Temperature, (b) total flow velocity, (c) advective component of the total velocity, and (d) thermal-osmotic component of the total velocity. Notice how the advective component of flow cancels the thermal-osmotic component, and there is no net effect of thermal osmosis on the flow field. The flow field is homogeneous, with fluid flowing in the y direction, down the overall hydraulic gradient.

6.2.2.2 Case 2 (T1 = 299.20 K, T2 = 298.10 K)

Figures 6.8, 6.9 and 6.10 show the results corresponding to sections of the flow domain perpendicular to the x, y, and z axes, respectively. The three sections intersect at the center of the flow domain.

A value of the hydraulic conductivity (K) equal to 10^{-7} m/s was used in this case, so the magnitudes of the components of the total flow velocity in the y and z directions were in principle the same, given the overall hydraulic and temperature gradients. Fluid should be expected to flow perpendicular to the x axis, and at an angle of 45° from both the y and z axis.

The results show that, effectively, water flows at a 45° angle between the y and z axes, down the hydraulic and temperature gradients, and perpendicular to the x axis. The advective component of flow cancels the thermal-osmotic component arising from the presence of a heat source in the center of the domain. The magnitude of the total flow velocity at all points is given by

$$v = \left(\left(-K \frac{\mathrm{h2} - \mathrm{h1}}{\mathrm{L_y}} \right)^2 + \left(-k_T \frac{\mathrm{T2} - \mathrm{T1}}{\mathrm{L_z}} \right)^2 \right)^{\frac{1}{2}}$$

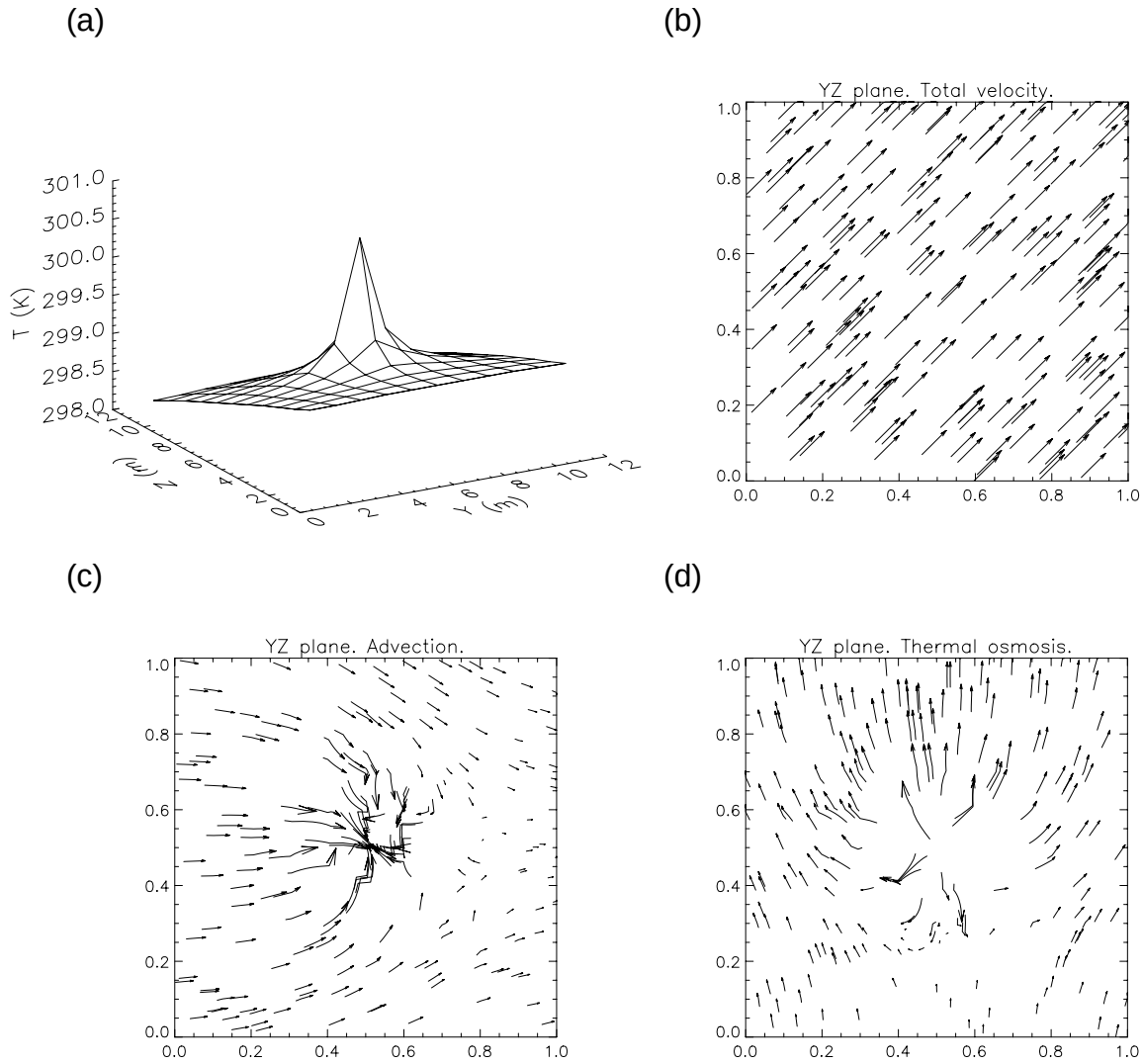

Figure 6.8: Results for case 2 (T1 = 299.20 K, T2 = 298.10 K) in a section of the flow domain perpendicular to the x axis and going through the center of the domain. (a) Temperature, (b) total flow velocity, (c) advective component of the total velocity, and (d) thermal-osmotic component of the total velocity. Notice how the advective component of flow cancels the thermal-osmotic component, and there is no net effect of thermal osmosis arising from the presence of a heat source in the interior of the domain. The flow field is homogeneous, with fluid flowing at a 45° angle between the y and z axes, perpendicular to the x axis, and down the overall hydraulic and thermal gradients.

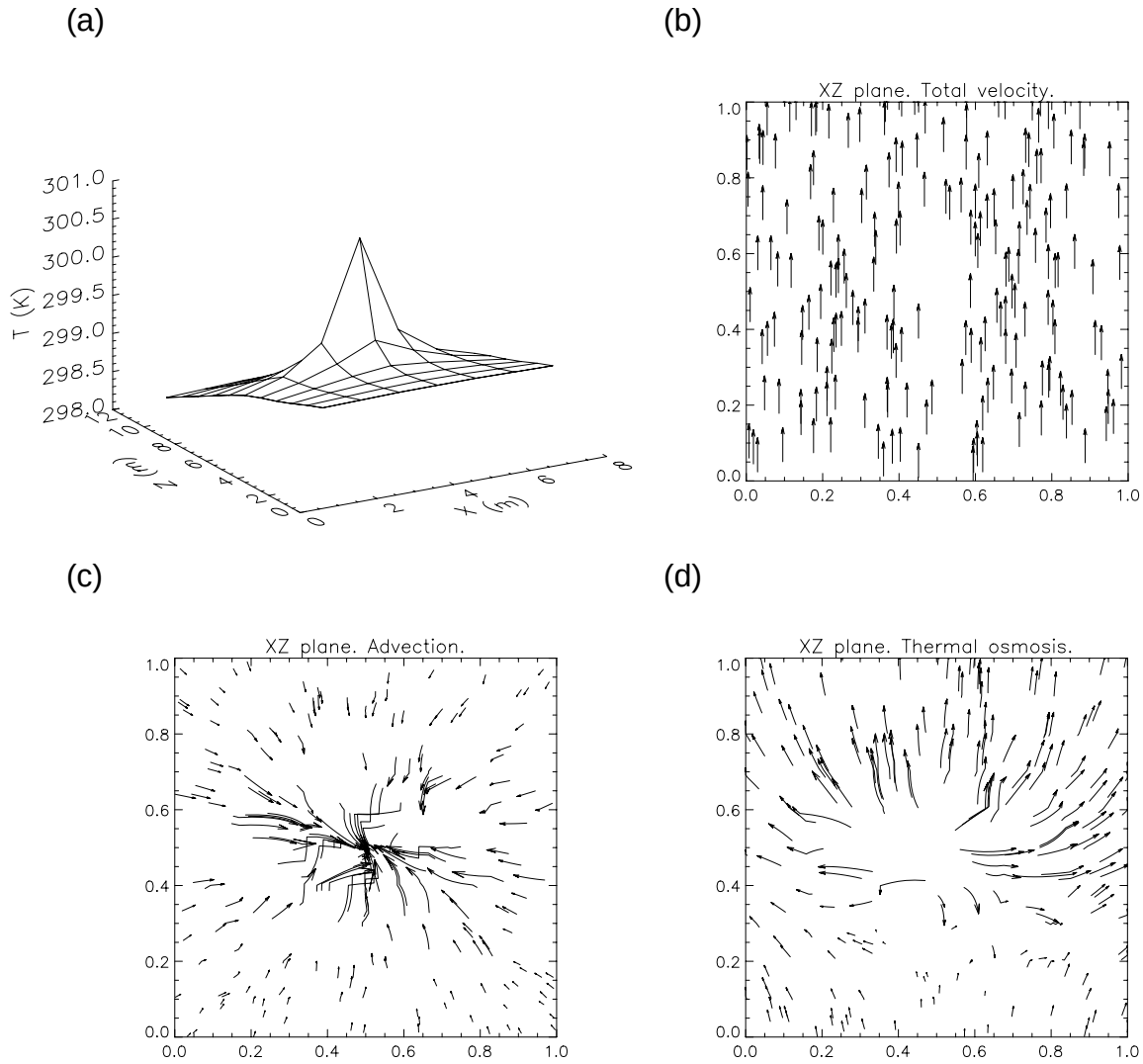

Figure 6.9: Results for case 2 (T1 = 299.20 K, T2 = 298.10 K) in a section of the flow domain perpendicular to the y axis and going through the center of the domain. (a) Temperature, (b) total flow velocity, (c) advective component of the total velocity, and (d) thermal-osmotic component of the total velocity. Notice how the advective component of flow cancels the thermal-osmotic component, and there is no net effect of thermal osmosis arising from the presence of a heat source in the interior of the domain. The flow field is homogeneous, with fluid flowing at a 45° angle between the y and z axes (parallel to the z axis in this section perpendicular to the y axis), and down the overall hydraulic and thermal gradients.

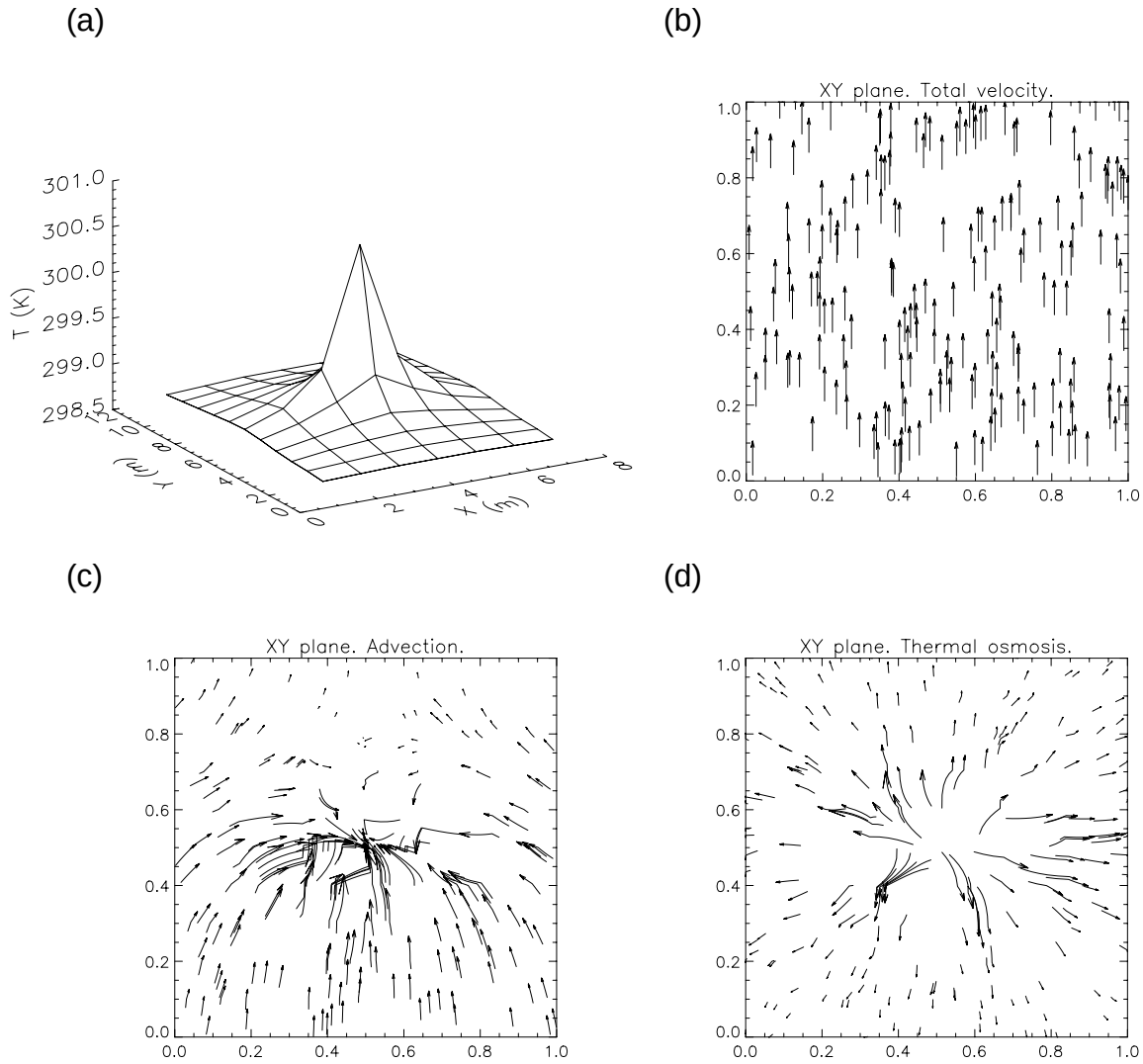

Figure 6.10: Results for case 2 (T1 = 299.20 K, T2 = 298.10 K) in a section of the flow domain perpendicular to the z axis and going through the center of the domain. (a) Temperature, (b) total flow velocity, (c) advective component of the total velocity, and (d) thermal-osmotic component of the total velocity. Notice how the advective component of flow cancels the thermal-osmotic component, and there is no net effect of thermal osmosis arising from the presence of a heat source in the interior of the domain. The flow field is homogeneous, with fluid flowing at a 45° angle between the y and z axes (parallel to the y axis in this section perpendicular to the z axis), and down the overall hydraulic and thermal gradients.

6.3 Two-dimensional model with temperature-dependent fluid density and viscosity

An additional two-dimensional model has been developed in order to evaluate the possible effects of temperature-dependent fluid density and viscosity in the calculations.

6.3.1 Model formulation

This new model is based on the two-dimensional model described in section 6.1, with the addition of the dependence of fluid density and viscosity on temperature. The model solves numerically the equations of conservation of fluid mass and conservation of energy, which are written now as

$$\nabla \cdot (\rho v) = 0 \tag{6.4}$$

and

$$\nabla \cdot \kappa \nabla T - c_f \nabla \cdot (\rho v T) + A = 0 \tag{6.5}$$

The total flow velocity or total specific discharge, v, is given by

$$v = -\frac{k}{\mu}(\nabla p + \rho g \nabla x) - k_T \nabla T \tag{6.6}$$

where the two terms on the right-hand-side of Eqn. 6.6 are the advective and thermal-osmotic components of the flow velocity. k is the permeability of the medium, μ is the viscosity of the fluid, and p is fluid pressure. Fluid pressure (p) and temperature (T) are the unknowns of this system of differential equations. Elevation has been defined to correspond to the x axis.

A simple linear dependence of fluid density on temperature has been used (see for instance FURBISH, 1997), with the form

$$\rho = \rho_0 (1 - \alpha (T - T_0)) \tag{6.7}$$

ρ_0, T_0, and α are the reference density, reference temperature, and coefficient of thermal expansion of water, respectively. A constant value of α equal to 3×10^{-4} K^{-1} (a reasonable assumption at temperatures between 25°C and 35°C; see LIDE, 1998) has been used.

The dependence of the viscosity of water on temperature used in the model is from the study by BRUGES, LATTO & RAY, 1966, and has the form

$$\mu = 239.4 \times 10^{-7} \times 10^{\frac{248.37}{T - 140.0}} \text{ kg/m/s} \tag{6.8}$$

The type of flow domain and boundary conditions used in the model are identical to the ones shown in Fig. 6.1, except for the fact that the unknowns are pressure (p) and temperature (T), instead of hydraulic head (h) and temperature (T).

6.3.2 Results and discussion

Only the results from one simulation will be shown in this section. The iterative solution scheme used to solve the equations (Newton's method) did not provide good convergence in many of the cases that were tried. However, the case that will be shown here converged properly and displayed the same kind of solution obtained in the previous sections. Notice that the values of permeability and thermo-osmotic permeability used in the simulation are higher than the corresponding values in the previous simulations. Again, the goal of the calculations is to show how the coupling between the two transport mechanisms works, rather than obtaining specific values for the flow velocities. Numerical difficulties are also the reason why three-dimensional simulations with temperature-dependent density and viscosity are not presented.

The parameters for the simulation that will be shown are:

L = 5 m; 0.2 m spacing between nodes

p1 = p2 = 10^5 Pa

T1 = T2 = 298.15 K

k = 10^{-14} m^2

k_T = 10^{-6} m^2/K/s

κ = 2.6 W/m/K

A = 40 J/m^3/s (only in one node at the center of the domain)

ρ_0 = 997.05 kg/m^3

T_0 = 298.15 K

c_f = 4180 J/kg/K

Notice that since the pressure at all boundaries is the same (p1 = p2), the overall hydraulic gradient is given by the buoyancy term in Darcy's law ($\rho g \nabla x$ in Eqn. 6.6), and the flow will be in the direction of decreasing x (elevation was defined to correspond to x).

Figure 6.11(a) shows the calculated temperature distribution in the system. Figures 6.11(b), 6.11(c), and 6.11(d) show the total flow velocity, the advective component of the total flow velocity, and the thermal-osmotic component, respectively. Notice that thermal osmosis promotes fluid transport down the temperature gradient (from the center of the domain outwards). Again, as in the results showed in the previous sections, the advective component of flow

cancels the thermal-osmotic component. The result is that there is no net effect of thermal osmosis, even with density and viscosity effects taken into account, and at least given the relatively low temperature gradients assumed to apply in this case. The total velocity field is homogeneous (no component of velocity in the y direction) and with no contribution from thermal osmosis.

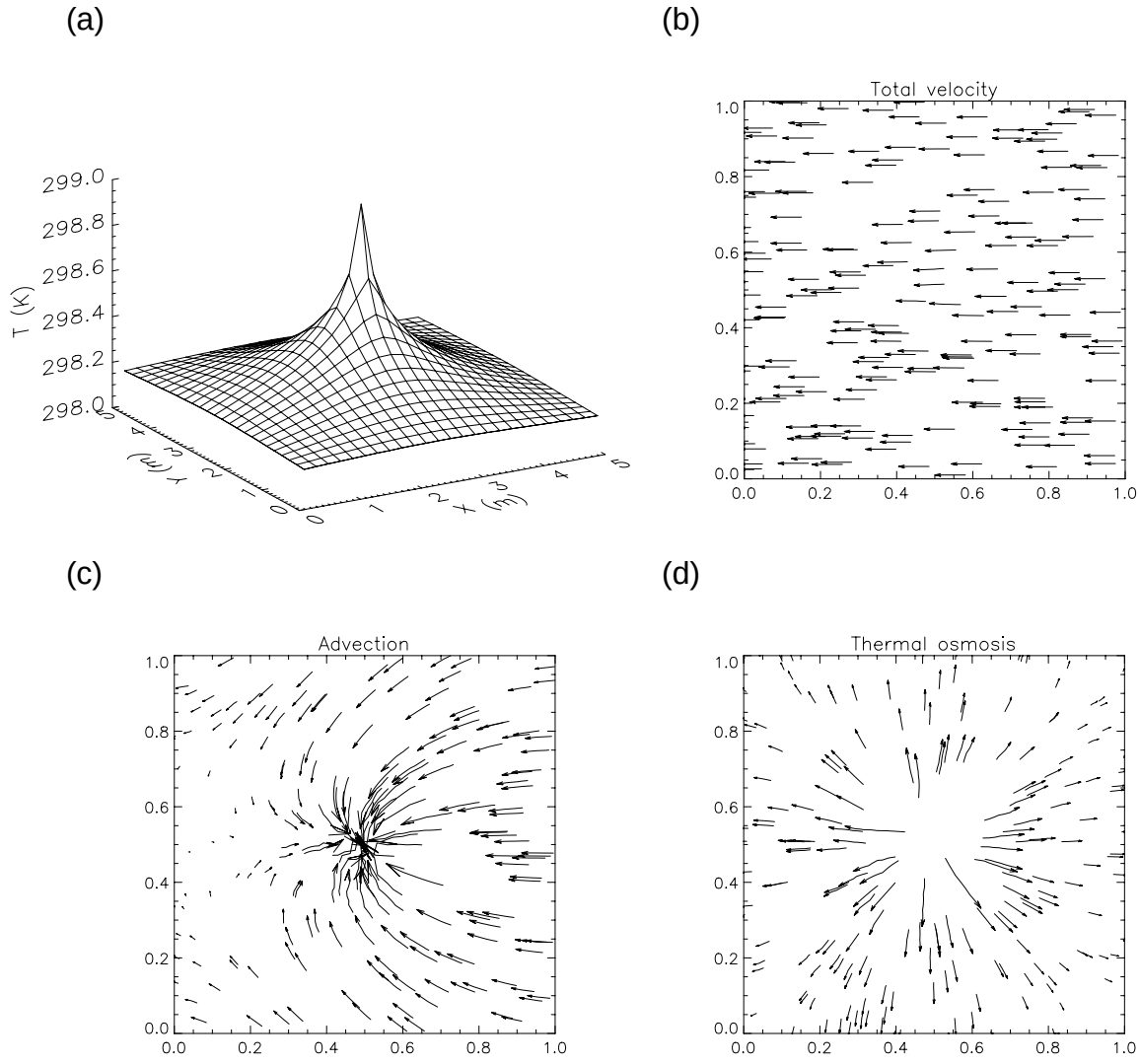

Figure 6.11: Results for the two-dimensional simulation with temperature-dependent density and viscosity. (a) Temperature, (b) total flow velocity, (c) advective component of the of the total velocity, and (d) thermal-osmotic component of the total velocity. Notice how the advective component of flow cancels the thermal-osmotic component, and there is no net effect of thermal osmosis on the flow field.

7. CONCLUSIONS

The objective of this study was to place some constraints on the potential effects of coupled phenomena on fluid, solute and heat transport in the vicinity of a repository for vitrified high-level radioactive waste (HLW) and spent nuclear fuel (SF) hosted by the Opalinus Clay (OPA), and in the context of a fully-saturated OPA at the time of waste canister failure ($t \approx 1000$ y).

-Firstly, estimates of the solute fluxes associated with chemical osmosis, hyperfiltration, thermal diffusion and thermal osmosis were calculated. Available experimental data concerning coupled transport phenomena in compacted clays, and the hydrogeological and geochemical conditions to which the Opalinus Clay is subject, were used for these estimates.

Hyperfiltration can only be as large in magnitude as advection, and it always acts in the opposite direction, suggesting that any contribution from such a transport mechanism would be beneficial for repository performance (against the release of radionuclides from the OPA).

Chemical-osmotic fluxes could be significant under some conditions but, for conditions similar to those in the Mont Terri Underground Rock Laboratory (high salinity in the OPA; low salinity outside), any chemical-osmotic flux would be directed towards the OPA, and therefore against any release of radionuclides from the OPA.

Thermal diffusion does not seem to contribute in a significant manner to solute fluxes, given the low temperature gradient conditions believed to apply to the vicinity of a HLW/SF repository at the time of waste canister failure.

Finally, and without taking conservation of fluid mass into account, thermal osmosis seems to be the only coupled transport mechanism that could potentially have a strong effect on fluid and solute transport in the vicinity of a repository hosted by the Opalinus Clay. However, there is a significant lack of data regarding thermo-osmotic permeabilities of clays, causing a high degree of uncertainty in such estimates.

-Secondly, estimates of the heat fluxes associated with thermal filtration and the Dufour effect in the vicinity of the repository were calculated. Due to the lack of experimental data, the phenomenological coefficients for these heat transport mechanisms were obtained by means of the Onsager Reciprocal Relations and the values for their conjugated coupled phenomena (thermal osmosis and thermal diffusion). The calculated heat fluxes are absolutely negligible compared to the heat fluxes caused by thermal conduction.

-As a further step to obtain additional insight into the effects of coupled phenomena on solute transport, the solute fluxes associated with advection, chemical diffusion, thermal and chemical osmosis, hyperfiltration and thermal diffusion were incorporated into a simple one-dimensional transport equation. Under the assumption of constant hydraulic, temperature and osmotic pressure head gradients, constant porosity, effective diffusion coefficient, hydraulic conductivity, osmotic efficiency, Soret coefficient and thermo-osmotic permeability, the equation has a simple analytical solution, which can be used to estimate the effects of direct and coupled transport phenomena. By making use of parameters intended to simulate the conditions in the vicinity of a repository for vitrified high-level waste and spent fuel hosted by the Opalinus Clay, the equation shows that thermal osmosis is the only coupled transport mechanism that could potentially have a strong effect on solute and fluid transport in the vicinity of the repository, supporting the results of the previous estimates.

-Finally, the results of two- and three-dimensional flow models incorporating advection (Darcy's law) and thermal osmosis, under conditions (temperature and hydraulic gradients) simulating the vicinity of the repository at the time of waste canister failure ($t \approx 1000$ y) and taking conservation of fluid mass and conservation of energy constraints into account, have shown that the advective component of the flow velocity cancels the thermal-osmotic component arising from the presence of a heat source in the interior of the flow domain. These simulations were run under the assumption of constant fluid density and viscosity.

Additional two-dimensional simulations with temperature-dependent density and viscosity have shown the same type of solution, with the advective component of flow cancelling the thermal-osmotic component (no net effect of thermal osmosis), at least under the low temperature gradients believed to apply in the vicinity of the repository at the time of waste canister failure. The fact that taking three-dimensional flow into account did not make any difference regarding the coupling between advection and thermal osmosis in the simulations with constant fluid density and viscosity suggests that the same type of coupling will apply to three-dimensional flow with temperature-dependent fluid density and viscosity.

-The main conclusion arising from this study is that coupled phenomena will only have a very minor impact on radionuclide transport in the Opalinus Clay, at least under the conditions at the expected time of waste canister failure (times equal to or greater than 1000 years). It would be advisable to guarantee the performance of the canisters up to these times through quality control. The

effects of coupled phenomena on solute, fluid and heat transport in the near field of the repository (bentonite buffer) and at time scales less than 1000 years will have to be addressed to achieve a full understanding of the role of coupled phenomena on the whole repository system.

8. ACKNOWLEDGEMENTS

Partial financial support by the Swiss National Cooperative for the Disposal of Radioactive Waste (Nagra), and the valuable comments from Urs Berner, Andreas Gautschi, Jörg Hadermann, Walter Heer, Andreas Jakob, Martin Mazurek, Joe Pearson, Jürg Schneider, and Piet Zuidema, are gratefully acknowledged. Acknowledgements are also due to Dr.. G. de Marsily and Dr. P. Jamet for their detailed review of the manuscript and helpful discussions.

9. REFERENCES

BARBOUR, S.L. & FREDLUND, D.G. (1989): Mechanisms of Osmotic Flow and Volume Change in Clay Soils. Can. Geotech. Jour. 26, 551-562.

BRUGES, E.A., LATTO, B. & RAY, A.K. (1966): New Correlations and Tables of the Coefficient of Viscosity of Water and Steam up to 1000 bar and 1000°C. Int. J. Heat Mass Transfer 9, 465-480.

CARNAHAN, C.L. (1984): Thermodynamic coupling of heat and matter flows in near-field regions of nuclear waste repositories. Mat. Res. Soc. Symp. Proc. 26, 1023-1030.

DIRKSEN, C. (1969): Thermo-Osmosis Through Compacted Saturated Clay Membranes. Soil Sci. Soc. Amer. Proc. 33, 821-826.

FURBISH, D.J. (1997): Fluid Physics in Geology. An Introduction to Fluid Motions on Earth's Surface and Within Its Crust. Oxford University Press, New York.

GARRELS, R.M. & CHRIST, C.L. (1965): Solutions, Minerals, and Equilibria. Harper and Row, New York.

GAUTSCHI, A. (1997): Hydrogeology of the Opalinus Clay - Implications for Radionuclide Transport. Nagra Bulletin 31, 24-32.

GAUTSCHI, A., ROSS, R. & SCHOLTIS, A. (1993): Pore Water - Groundwater Relationships in Jurassic Shales and Limestones of Northern Switzerland. In D.A.C. Manning, P.L. Hall & C.R. Hughes, eds., Geochemistry of Clay - Pore Fluid Interaction. Mineralogical Society Series 4, 412-422.

GROENEVELT, P.H., ELRICK, D.E. & LARYEA, K.B. (1980): Coupling Phenomena in Saturated Homo-Ionic Montmorillonite: IV. The Dispersion Coefficient. Soil Sci. Soc. Am. J. 44, 1168-1173.

DE GROOT, S.R. & MAZUR, P. (1962): Non-Equilibrium Thermodynamics. North-Holland, Amsterdam. Republished in 1984 by Dover, New York.

HARRINGTON, J.F. & HORSEMAN, S.T. (1999): Laboratory Experiments on Hydraulic and Osmotic Flow. In: M. Thury & P. Bossart, eds., Mont Terri Project: Results of the Hydrogeological, Geochemical and Geotechnical Experiments Performed in the Opalinus Clay (1996 - 1997). Swiss National Hydrological and Geological Survey Report, Bern (in preparation).

HORSEMAN, S.T., HIGGO, J.J.W., ALEXANDER, J. & HARRINGTON, J.F. (1996): Water, Gas and Solute Movement Through Argillaceous Media. NEA-OECD Report CC-96/1.

KATCHALSKY, A. & CURRAN, P.F. (1965): Nonequilibrium Thermodynamics in Biophysics. Harvard University Press, Cambridge.

KEMPER, W.D. & EVANS, N.A. (1963): Movement of Water as Effected by Free Energy and Pressure Gradients III. Restriction of Solutes by Membranes. Soil Sci. Soc. Am. Proc. 27, 485-490.

KEMPER, W.D. & ROLLINS, J.B. (1966): Osmotic Efficiency Coefficients Across Compacted Clays. Soil Sci. Soc. Am. Proc. 30, 529-534.

LASAGA, A.C. (1998): Kinetic Theory in the Earth Sciences. Princeton University Press, Princeton.

LERMAN, A. (1979): Geochemical Processes. Water and Sediment Environments. John Wiley and Sons, New York.

LI, Y.H. & GREGORY, S. (1974): Diffusion of Ions in Sea Water and in Deep-Sea Sediments. Geochim. Cosmochim. Acta 38, 703-714.

LIDE, D.R., ed. (1998): CRC Handbook of Chemistry and Physics. 79th edition. CRC Press, Boca Raton.

MARINE, I.W. & FRITZ, S.J. (1981): Osmotic Model to Explain Anomalous Heads. Water Resources Research 17, 73-82.

DE MARSILY, G., FARGUE, D. & GOBLET, P. (1987): How Much Do We Know About Coupled Transport Processes in the Geosphere and Their Relevance to Performance Assessment ? Proc. Geoval 1987, 475-491.

MAZUREK, M. (1999): Mineralogy of the Opalinus Clay. In: M. Thury & P. Bossart, eds., Mont Terri Project: Results of the Hydrogeological, Geochemical and Geotechnical Experiments Performed in the Opalinus Clay (1996 - 1997). Swiss National Hydrological and Geological Survey Report, Bern (in preparation).

NAGRA (1984): Die Kernbohrung Beznau. Nagra Technischer Bericht 84-34.

NAGRA (1989a): Sedimentstudie - Zwischenbericht 1988. Möglichkeiten zur Endlagerung Langlebiger Radioaktiver Abfälle in den Sedimenten der Schweiz. Nagra Technischer Bericht 88-25. Also executive summary in English, Nagra Technical Report 88-25E.

NAGRA (1989b): Sondierbohrung Weiach - Untersuchungsbericht. Nagra Technischer Bericht 88-08.

NAGRA (1994): Sedimentstudie - Zwischenbericht 1993: Zusammenfassende Uebersicht der Arbeiten von 1990 bis 1994 und Konzept für weitere Untersuchungen. Nagra Technischer Bericht 94-10.

OGATA, A. & BANKS R.B. (1961): A Solution of the Differential Equation of Longitudinal Dispersion in Porous Media. USGS Professional Paper 411-A.

ONSAGER, L. (1931): Reciprocal Relations in Irreversible Processes, II. Physical Review 38, 2265-2279.

PEARSON, F.J., SCHOLTIS, A., GAUTSCHI, A., BAEYENS, B., BRADBURY, M. & DEGUELDRE, C. (1999): Chemistry of Porewater. In: M. Thury & P. Bossart, eds., Mont Terri Project: Results of the Hydrogeological, Geochemical and Geotechnical Experiments Performed in the Opalinus Clay (1996 - 1997). Swiss National Hydrological and Geological Survey Report, Bern (in preparation).

SATO, R., SASAKI, T., ANDO, K., SMITH, P.A. & SCHNEIDER, J.W. (1998): Calculations of the Temperature Evolution of a Repository for Spent Fuel in Crystalline and Sedimentary Host Rocks. Nagra Technical Report 97-02.

SOLER, J.M. (1997): First Estimates of Solute Fluxes Associated with Coupled Transport Phenomena in the Opalinus Clay. PSI Internal Technical Report TM 44-97-13. Also published in PSI Annual Report 1997, Annex IV, 73-80.

SOLER, J.M. (1998a): Simple One-Dimensional Transport Simulations Including Thermal and Chemical Osmosis, Hyperfiltration, and Thermal Diffusion. PSI Internal Technical Report TM 44-98-04.

SOLER, J.M. (1998b): Estimates of the Heat Fluxes Associated with Thermal Filtration and the Dufour Effect in the Opalinus Clay. PSI Internal Technical Report TM 44-98-05.

SOLER, J.M. (1998c): Coupling Between Advection and Thermal Osmosis: Two-Dimensional Flow Calculations. PSI Internal Technical Report TM 44-98-10.

SOLER, J.M. & JAKOB, A. (1997): Formulation of a Solute Transport Equation Including the Effects of Coupled Phenomena. PSI Internal Technical Report TM 44-97-09.

SRIVASTAVA R.C. & AVASTHI, P.K. (1975): Non-equilibrium Thermodynamics of Thermo-Osmosis of Water Through Kaolinite. Journal of Hydrology 24, 111-120.

STUMM, W. & MORGAN, J.J. (1996): Aquatic Chemistry: Chemical Equilibria and Rates in Natural Waters. 3rd Edition. John Wiley and Sons, New York.

THORNTON, E.C. & SEYFRIED JR., W.E (1983): Thermodiffusional Transport in Pelagic Clay: Implications for Nuclear Waste Disposal in Geological Media. Science 220, 1156-1158.

THURY, M. (1997): The Mont Terri Rock Laboratory. Nagra Bulletin 31, 33-44.

ULLMAN, W.J. & ALLER, R.C. (1982): Diffusion Coefficients in Nearshore Marine Sediments. Limnology and Oceanography 27, 552-556.

DE WINDT, L. & PALUT, J.M. (1999): Tracer Feasibility Experiment (FM-C, DI). In: M. Thury & P. Bossart, eds., Mont Terri Project: Results of the Hydrogeological, Geochemical and Geotechnical Experiments Performed in the Opalinus Clay (1996 - 1997). Swiss National Hydrological and Geological Survey Report, Bern (in preparation).

WYSS, E., MARSCHALL, P. & ADAMS, J. (1999): Hydro- and Gas Testing (GP): Hydraulic Parameters and Formation Pressures in Matrix and Faults. In: M. Thury & P. Bossart, eds., Mont Terri Project: Results of the Hydrogeological, Geochemical and Geotechnical Experiments Performed in the Opalinus Clay (1996 - 1997). Swiss National Hydrological and Geological Survey Report, Bern (in preparation).

10. LIST OF SYMBOLS

A: Heat source term (J/m^3/s)

a_w: Activity of water (dimensionless)

c_i: Concentration of species i (kg/m^3)

c_f: Heat capacity of fluid at constant pressure (J/kg/K)

c_{tot}: Total solute concentration (kg/m^3)

D: Diffusion coefficient as used in the 1D transport equation (m^2/s)

D_0: Diffusion coefficient in water (m^2/s)

D_e: Effective diffusion coefficient (m^2/s)

F: Formation factor (dimensionless)

g: Gravitational acceleration (m/s^2)

h: Hydraulic head (m)

h': $\nabla h' = \nabla p + \rho g \nabla z$ (N/m^3)

J_{ADV}: Advective solute flux (kg/m^2/s)

J_{CO}: Chemical-osmotic solute flux (kg/m^2/s)

J_D: Chemical-diffusive solute flux (kg/m^2/s)

J_{DE}: Heat flux caused by Dufour effect (J/m^2/s)

J_{HYP}: Hyperfiltration solute flux (kg/m^2/s)

J_i: Generalized flux

J_i: Total mass flux of species i (kg/m^2/s)

J_i^0: "Dispersive" mass flux of species i (kg/m^2/s), arising from thermal diffusion, hyperfiltration, and chemical diffusion. $J_i = J_i^0 + c_i J_v$

J_q: Total heat flux (J/m^2/s)

J_q^0: Heat flux arising from thermal conduction, thermal filtration, and Dufour effect $J_q = J_q^0 + \rho c_f T J_v$ (J/m^2/s)

J_s: Flux of entropy driven by a temperature gradient (J/K/m^2/s)

J_{TC}: Thermal conduction heat flux (J/m^2/s)

J_{TD}: Thermal-diffusive solute flux (kg/m^2/s)

J_{TF}: Thermal filtration heat flux (J/m^2/s)

J_{TO}: Thermal-osmotic solute flux (kg/m^2/s)

J_v: Flux of fluid (m/s)

k: Permeability (m^2)

k_T: Thermo-osmotic permeability (m^2/K/s)

K: Hydraulic conductivity (m/s)

K_π: Coefficient of osmotic permeability (m/s)

L: Reference length (m)

$L_{ii}, L_{ij}, L'_{ii}, L'_{ij}$: Phenomenological coefficients

L_{ik}: Phen. coeff. for diffusion (kg·s·K/m^3)

L'_{ik}: Phen. coeff. for diffusion (kg·s/m^3)

L_{iq}: Phen. coeff. for thermal diffusion (kg·K/m/s)

L'_{iq}: Phen. coeff. for thermal diffusion (kg/K/m/s)

L_{iv}: Phen. coeff. for hyperfiltration (s·K)

L'_{iv}: Phen. coeff. for hyperfiltration (s)

L_{qk}: Phen. coeff. for Dufour effect (kg·K/m/s)

L'_{qk}: Phen. coeff. for Dufour effect (kg/K/m/s)

L_{qq}: Phen. coeff. for thermal conduction (J·K/m/s)

L'_{qq} : Phen. coeff. for thermal conduction ($J/K^2/m/s$)

L_{qv} : Phen. coeff. for thermal filtration ($m^2 K/s$)

L'_{qv} : Phen. coeff. for thermal filtration ($m^2/K/s$)

L_{vk} : Phen. coeff. for chemical osmosis ($s K$)

L'_{vk} : Phen. coeff. for chemical osmosis (s)

L_{vq} : Phen. coeff. for thermal osmosis ($m^2 K/s$)

L'_{vq} : Phen. coeff. for thermal osmosis ($m^2/K/s$)

L_{vv} : Phen. coeff. for advection ($m^3 s K/kg$)

L_{vv} : Phen. coeff. for advection ($m^3 s/kg$)

$L_{Pe=1}$: Reference length (m) for $Pe = 1$

m : Cementation exponent (dimensionless)

p : Fluid pressure (Pa)

Pe : Peclet number (dimensionless)

R : Gas constant (J/mol/K)

s : Soret coefficient (K^{-1})

S : Entropy (J/K)

t : Time (s)

T : Temperature (K)

T_0 : Reference temperature (K)

v : Velocity-like term in the 1D transport equation (m/s)

v : Total flow velocity (m/s)

v_{CO} : Chemical-osmotic flux of fluid (m/s)

v_D : Darcy velocity (m/s)

v_{TO} : Thermal-osmotic flux of fluid (m/s)

V : Volume (m^3)

V_w : Molar volume of water (m^3/mol)

W_k : Molar weight of species k (kg/mol)

$\overline{W}$: Average molar weight (kg/mol)

x : Distance (m)

X_j : Generalized driving force

y : Distance (m)

z : Distance (m)

α : Coefficient of thermal expansion (K^{-1})

χ : Constrictivity (dimensionless)

ϕ : Porosity (dimensionless)

κ : Thermal conductivity (W/m/K)

μ : Viscosity of fluid (kg/m/s)

μ_k : Concentration- and temperature-dependent part of the chemical potential of species k (J/mol)

Π : Osmotic pressure (Pa) $\Pi = -\frac{RT}{V_w}\ln a_w$

Π_h : Osmotic pressure head (m) $\Pi_h = \frac{\Pi}{\rho g}$

ρ : Density of fluid (kg/m^3)

ρ_0 : Reference density (kg/m^3)

σ : Coefficient of osmotic efficiency (dimensionless)

τ : Tortuosity (dimensionless)